
ACE - European School of Antennas

“High-frequency techniques and travelling wave antennas”

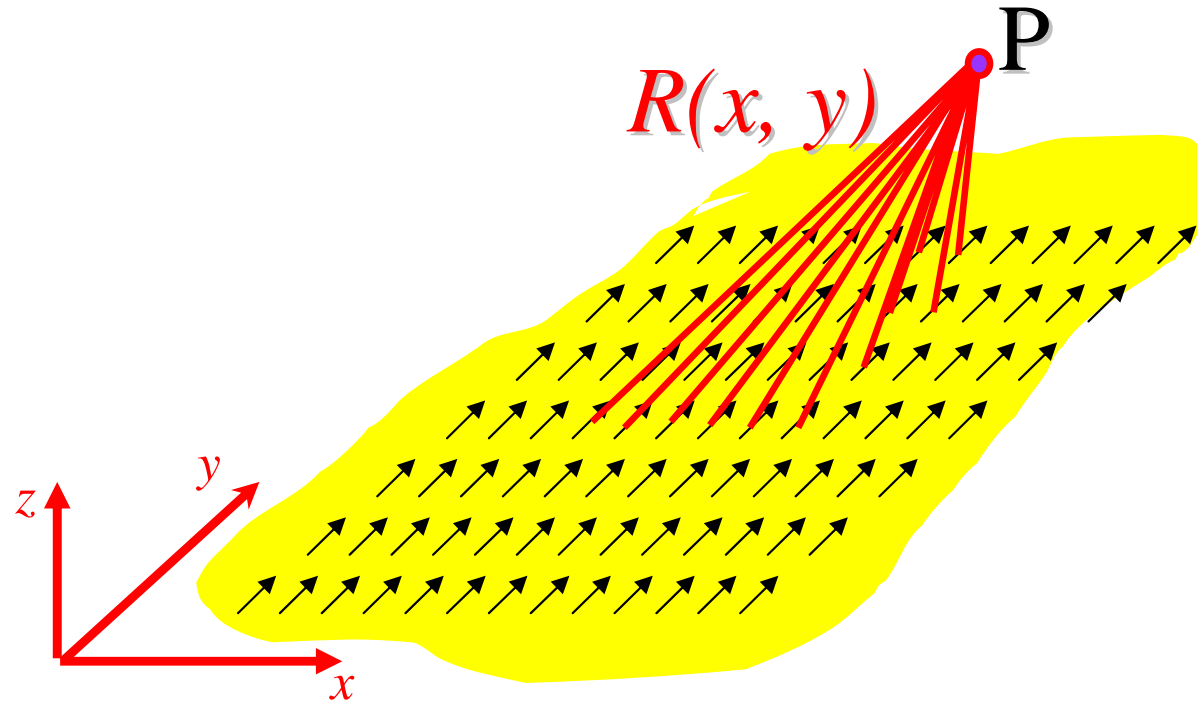
Siena – Roma, February 21 – 26, 2005

Truncated FW diffraction and interaction with complex platforms



GREEN'S FUNCTION FOR A PHASED ARRAY OF DIPOLES

- INFINITE ARRAY GF: ELEMENT BY ELEMENT SUMMATION



$$A(P) = \sum_{n=-\infty}^{+\infty} \sum_{m=-\infty}^{+\infty} g(P; nd_x, md_y) e^{-j(k_{x0}nd_x + k_{y0}md_y)}$$

$g(P; x, y)$ Green's function for the single dipole

Example: in free space

$$g(P; x, y) = \frac{e^{-jkR(x,y)}}{4\pi R(x,y)}$$

👉 Slowly convergent representation

GREEN'S FUNCTION FOR A PHASED ARRAY OF DIPOLES

- INFINITE ARRAY GF: FLOQUET WAVE EXPANSION

$$A(P) = \sum_{n=-\infty}^{+\infty} \sum_{m=-\infty}^{+\infty} g(P; nd_x, md_y) e^{-j(k_{x0}nd_x + k_{y0}md_y)} = \frac{1}{d_x d_y} \sum_{q=-\infty}^{+\infty} \sum_{p=-\infty}^{+\infty} G(\underline{k}_{pq}^{FW}) e^{-j\underline{k}_{pq}^{FW} \cdot \underline{r}}$$

$$g(P; x, y) = \frac{1}{4\pi^2} \int_{-\infty}^{+\infty} \int_{-\infty}^{+\infty} G(\underline{k}) e^{-j\underline{k} \cdot \underline{r}} d\underline{k}_x d\underline{k}_y$$

$$G(\underline{k}) e^{-j\underline{k} \cdot \underline{r}} = \int_{-\infty}^{+\infty} \int_{-\infty}^{+\infty} g(P; x, y) e^{-j\underline{k} \cdot \underline{R}} dx dy$$

$$\sum_{n=-\infty}^{+\infty} f(nd) = \frac{1}{d} \sum_{p=-\infty}^{+\infty} \int_{-\infty}^{+\infty} f(z) e^{-j\frac{2\pi p}{d}z} dz$$

Poisson summation formula

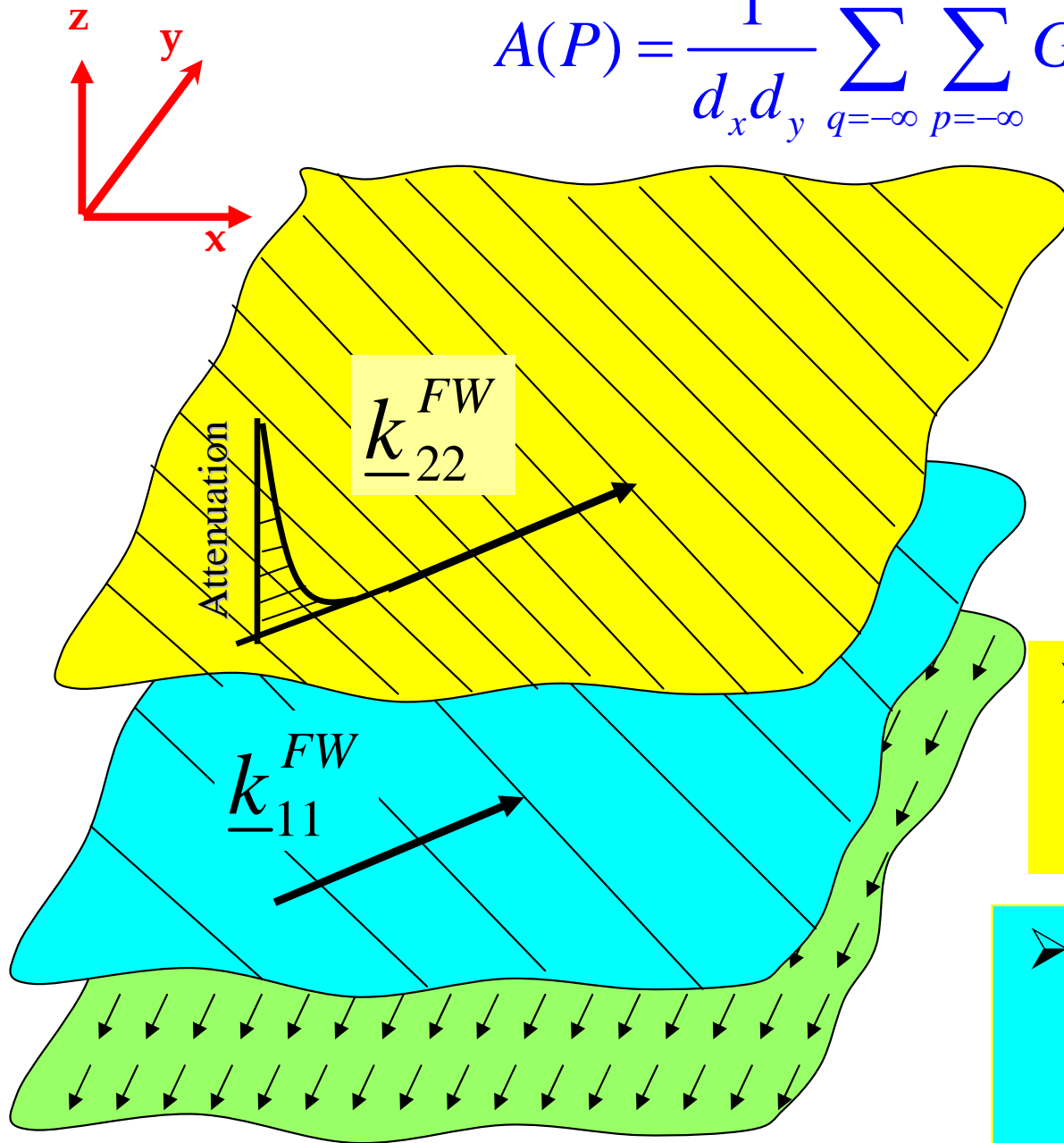
$$\underline{k}_{pq}^{FW} = k_{xp} \hat{x} + k_{yq} \hat{y} + k_{zpq} \hat{z}$$

$$p, q = 0, \pm 1, \pm 2, \dots$$

$$\left\{ \begin{array}{l} k_{xp} = k_{x0} + \frac{2\pi p}{d_x} \\ k_{yq} = k_{y0} + \frac{2\pi q}{d_y} \\ k_{zpq} = \sqrt{k^2 - k_{xp}^2 - k_{yq}^2} = \sqrt{k^2 - k_{\rho pq}^2} \end{array} \right.$$

GREEN'S FUNCTION FOR A PHASED ARRAY OF DIPOLES

$$A(P) = \frac{1}{d_x d_y} \sum_{q=-\infty}^{+\infty} \sum_{p=-\infty}^{+\infty} G(\underline{k}_{pq}^{FW}) e^{-j \underline{k}_{pq}^{FW} \cdot \underline{r}}$$



➤ EFW: *Evanescent Floquet waves*

$$k_{zpq} \in \mathbb{C}, \quad k_{\rho pq}^2 > k^2$$

➤ PFW: *Propagating Floquet waves*

$$k_{zpq} > 0, \quad k_{\rho pq}^2 < k^2$$

GREEN'S FUNCTION FOR A PHASED ARRAY OF DIPOLES

• TRUNCATED ARRAY GF

The periodicity is broken \Rightarrow the FW basis is not complete

$$\sum_{n=0}^{+\infty} f(nd) = \frac{1}{2} f(0) + \frac{1}{d} \sum_{p=-\infty}^{+\infty} \int_0^{+\infty} f(z) e^{-j\frac{2\pi p}{d}z} dz$$

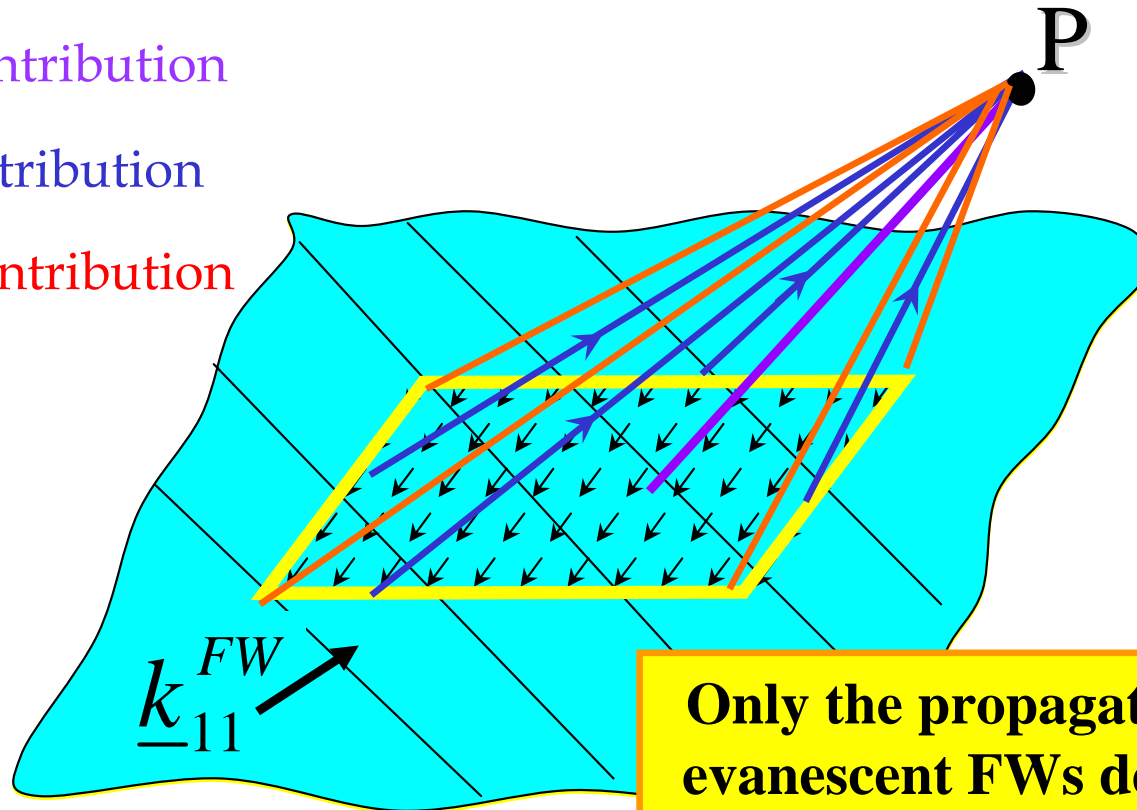
Truncated Poisson summation formula

Radiation integral on the truncated domain

Stationary phase contribution

Edge-end-point contribution

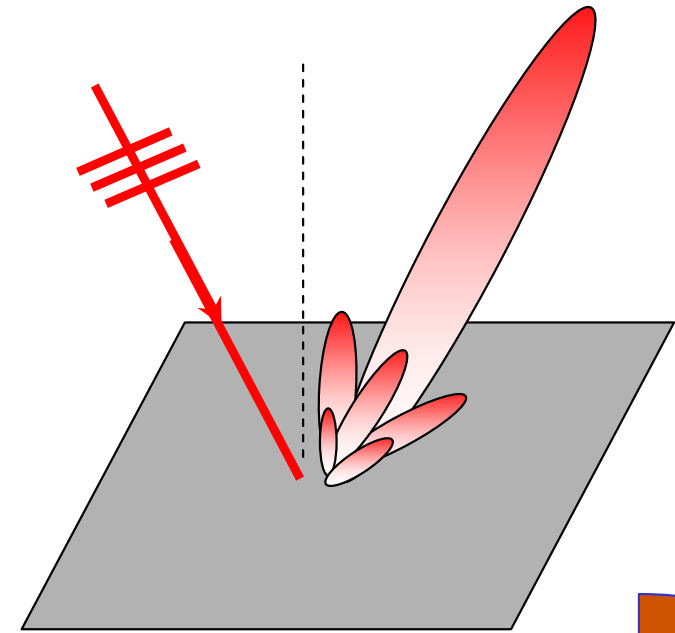
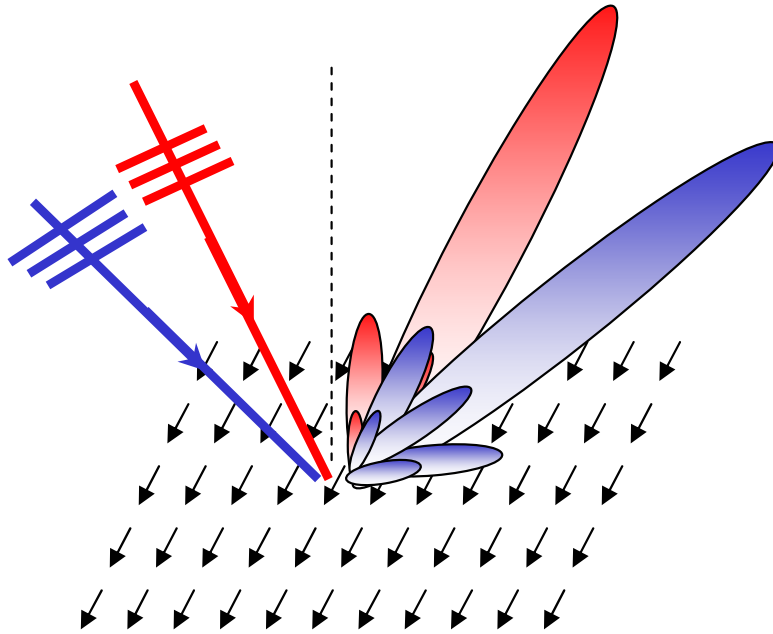
Vertex end-point contribution



Only the propagating and the first evanescent FWs describes the field accurately in most the cases

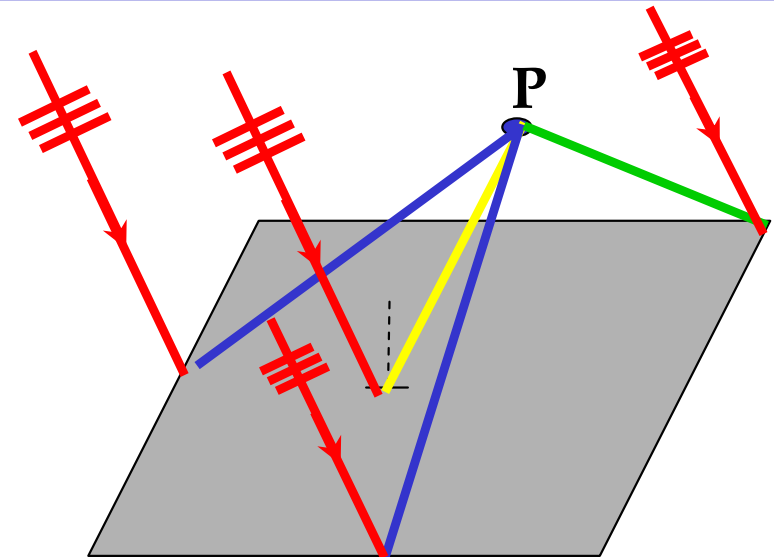
GREEN'S FUNCTION FOR A PHASED ARRAY OF DIPOLES

Array in free space: equivalence with far field scattering by a metallic plate



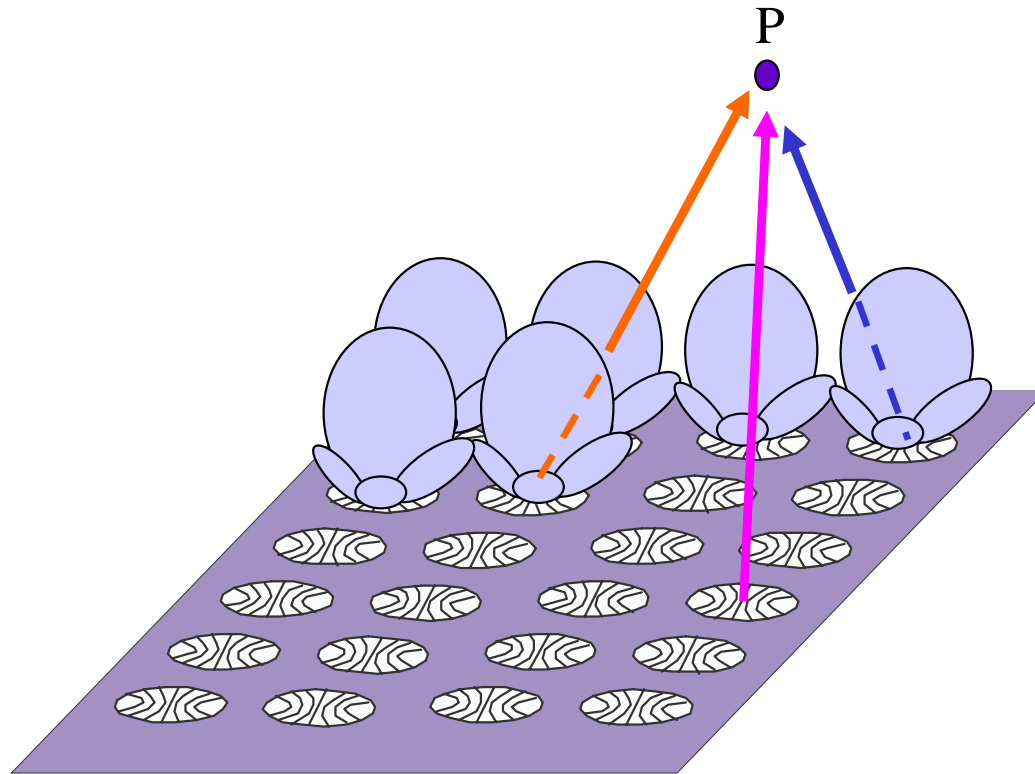
In the far zone, the radiation integral of each propagating FW produces a beam in the specular direction

Generalization to observation point at finite distance: UTD

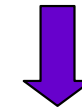


MOTIVATION: INTERACTION WITH THE ENVIRONMENT

In the far field of the single element
the momentum of each subcell can be replaced by the element factor



ARRAY Green's function
×
Element pattern



Generalization of the
LAW
ARRAY FACTOR
×
ELEMENT FACTOR
in the FRESNEL zone

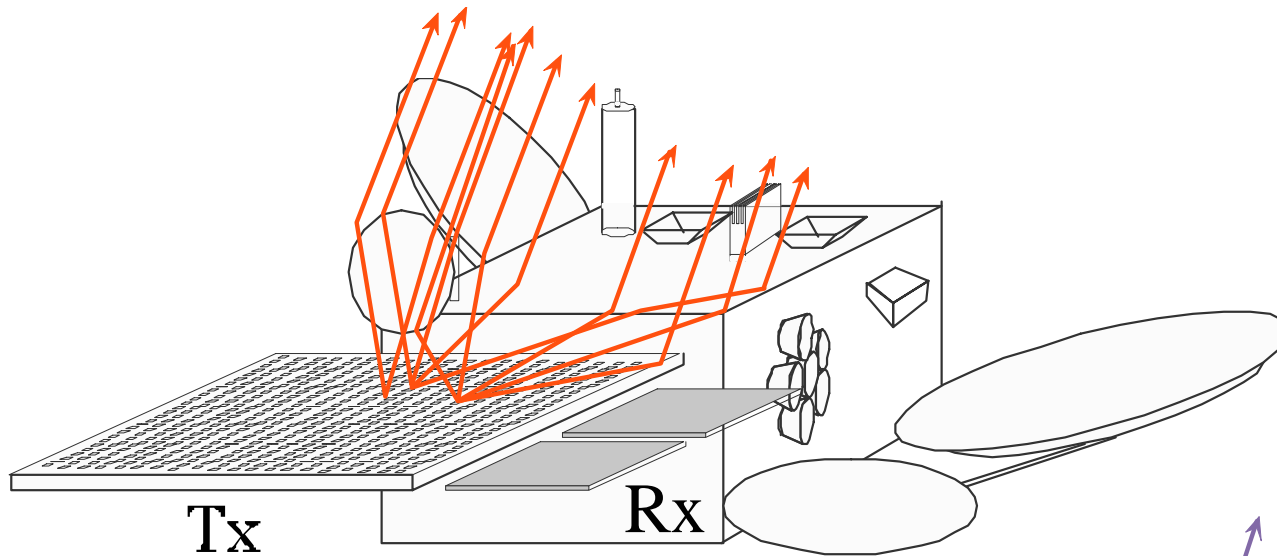
The radiation in the Fresnel zone from an array of arbitrary elements can be obtained by weighting each contribution by the proper element factor.

MOTIVATION: INTERACTION WITH THE ENVIRONMENT

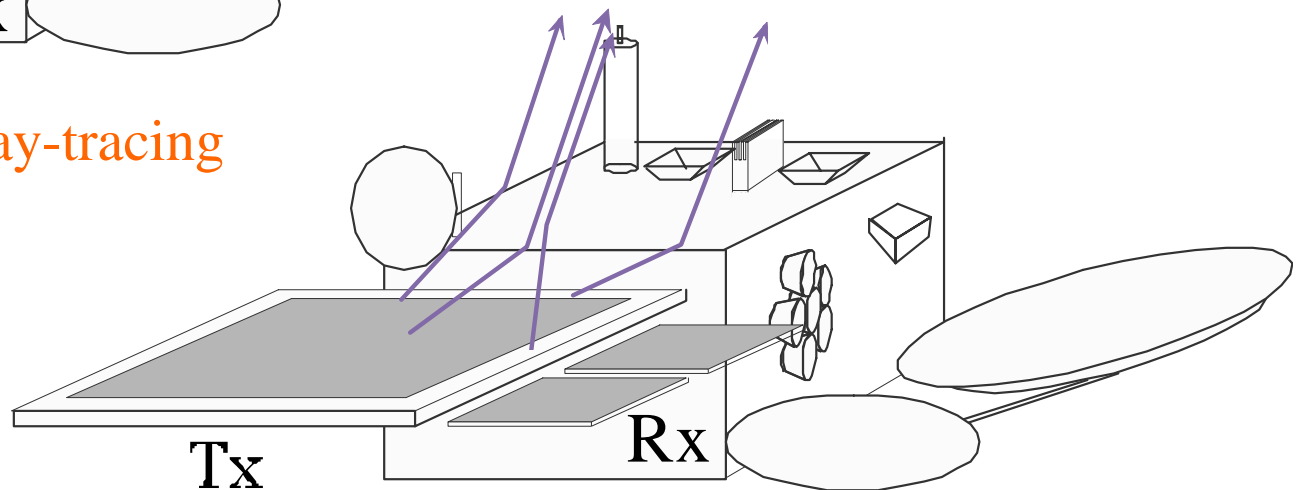
The radiation from the array can be collectively described in terms of a few rays associated to the FW of the infinite structure



efficient representation of the interaction with a complex environment

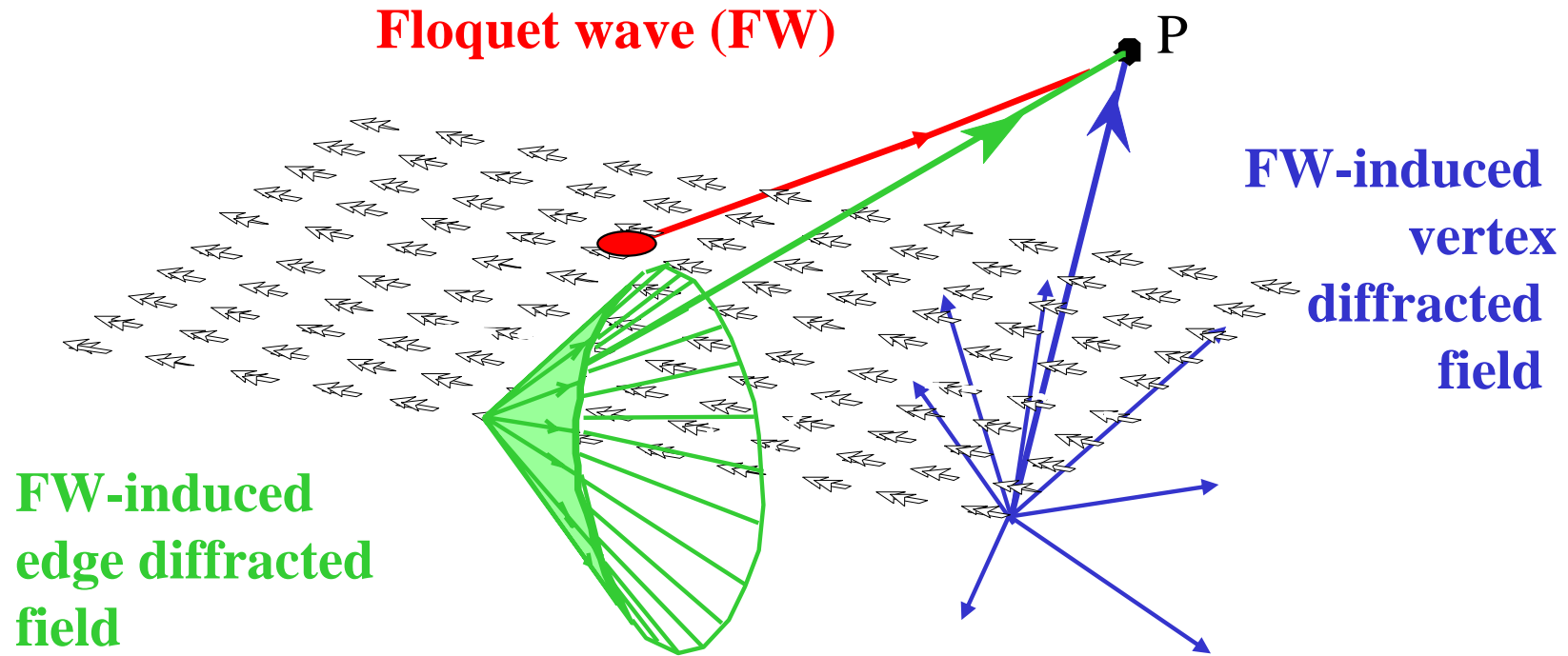


Element by element ray-tracing



Global TFW ray-tracing

RECTANGULAR ARRAY OF DIPOLES IN FREE SPACE



$$\mathbf{E} \approx \sum_{p,q} \mathbf{E}_{pq}^{FW} + \sum_{p,q} \mathbf{E}_{pq}^e + \sum_{p,q} \mathbf{E}_{pq}^v$$

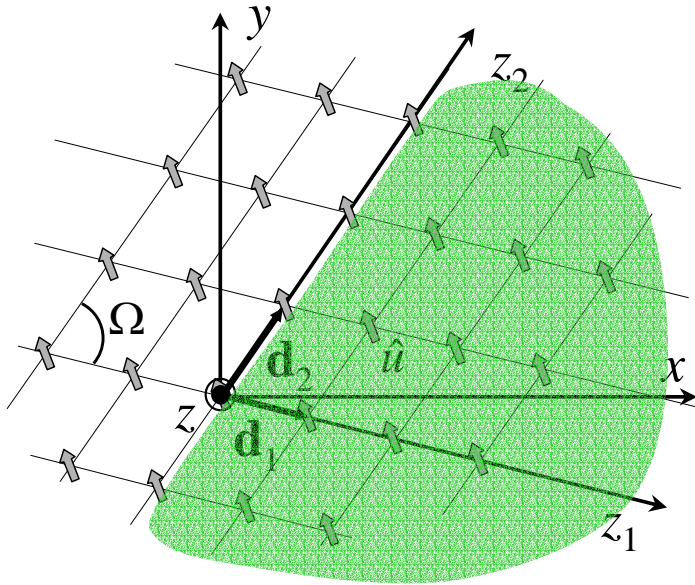
$$\mathbf{E}_{pq}^{FW} \approx U_{pq}^{FW} e^{-j\mathbf{k}_{pq}^{FW} \cdot \mathbf{r}}$$

$$\mathbf{E}_{pq}^e \approx U_{pq}^e \frac{e^{-j\mathbf{k}^e \cdot \mathbf{r}}}{\sqrt{k\rho}} + O((k\rho)^{-3/2})$$

$$\mathbf{E}_{pq}^v \approx \frac{e^{-jkr}}{kr} + O((kr)^{-2})$$

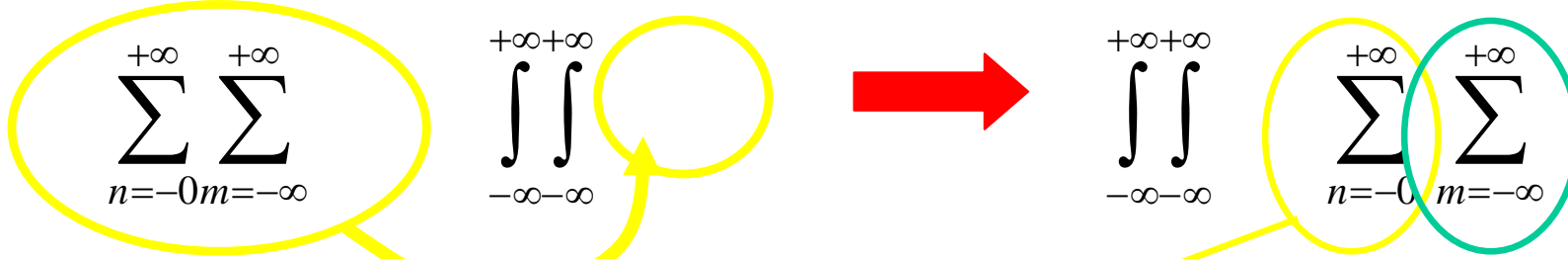
RECTANGULAR ARRAY OF DIPOLES IN FREE SPACE

CANONICAL PROBLEM FOR EDGE DIFFRACTION: SEMI-INFINITE ARRAY



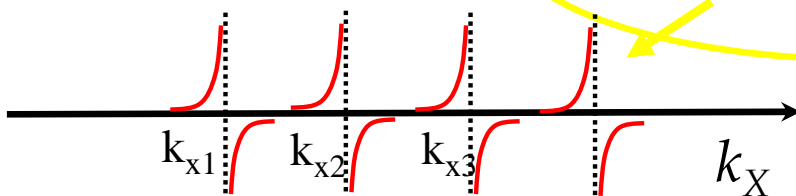
$$A(P) = \sum_{n=0}^{+\infty} \sum_{m=-\infty}^{+\infty} g(P; nd_x, md_y) e^{-j(k_{x0}nd_x + k_{y0}md_y)}$$

$$g(P; x, y) = \frac{\exp[-jkR(x, y)]}{R(x, y)} = \frac{1}{(2\pi)^2} \iint_{-\infty}^{+\infty} G(\underline{k}) e^{-j\vec{k} \cdot (\vec{r} - \vec{r}')} dk_x dk_y$$



$$k_{xp} = k_{x0} + \frac{2\pi p}{d_x}$$

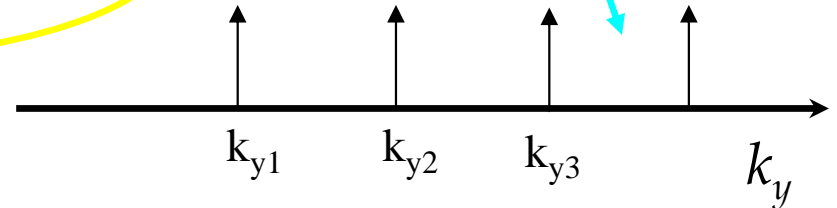
Train of Poles



$$B(k_x) = \frac{1}{1 - e^{j(k_x - k_{x0})d_x}}$$

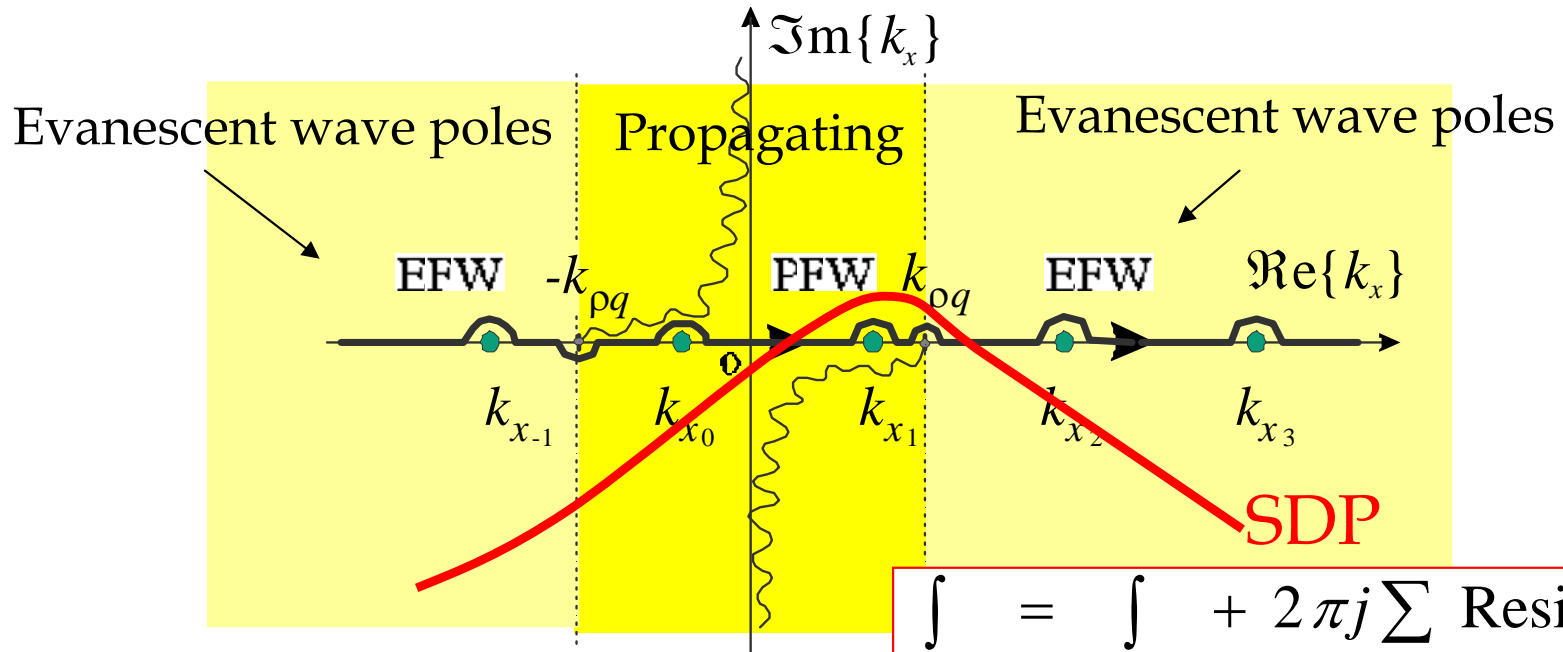
$$k_{yq} = k_{y0} + \frac{2\pi q}{d_y}$$

Train of Dirac delta functions

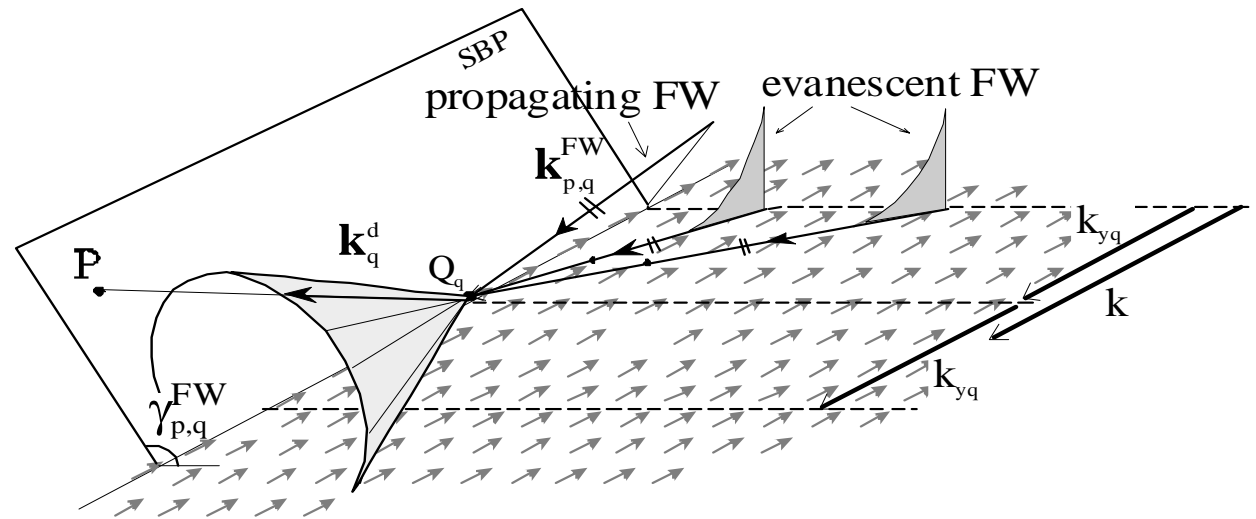
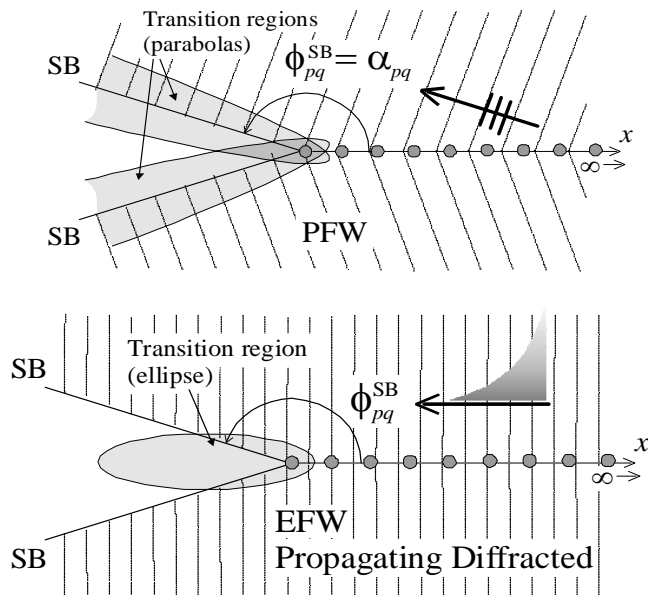


RECTANGULAR ARRAY OF DIPOLES IN FREE SPACE

CANONICAL PROBLEM FOR EDGE DIFFRACTION: SEMI-INFINITE ARRAY

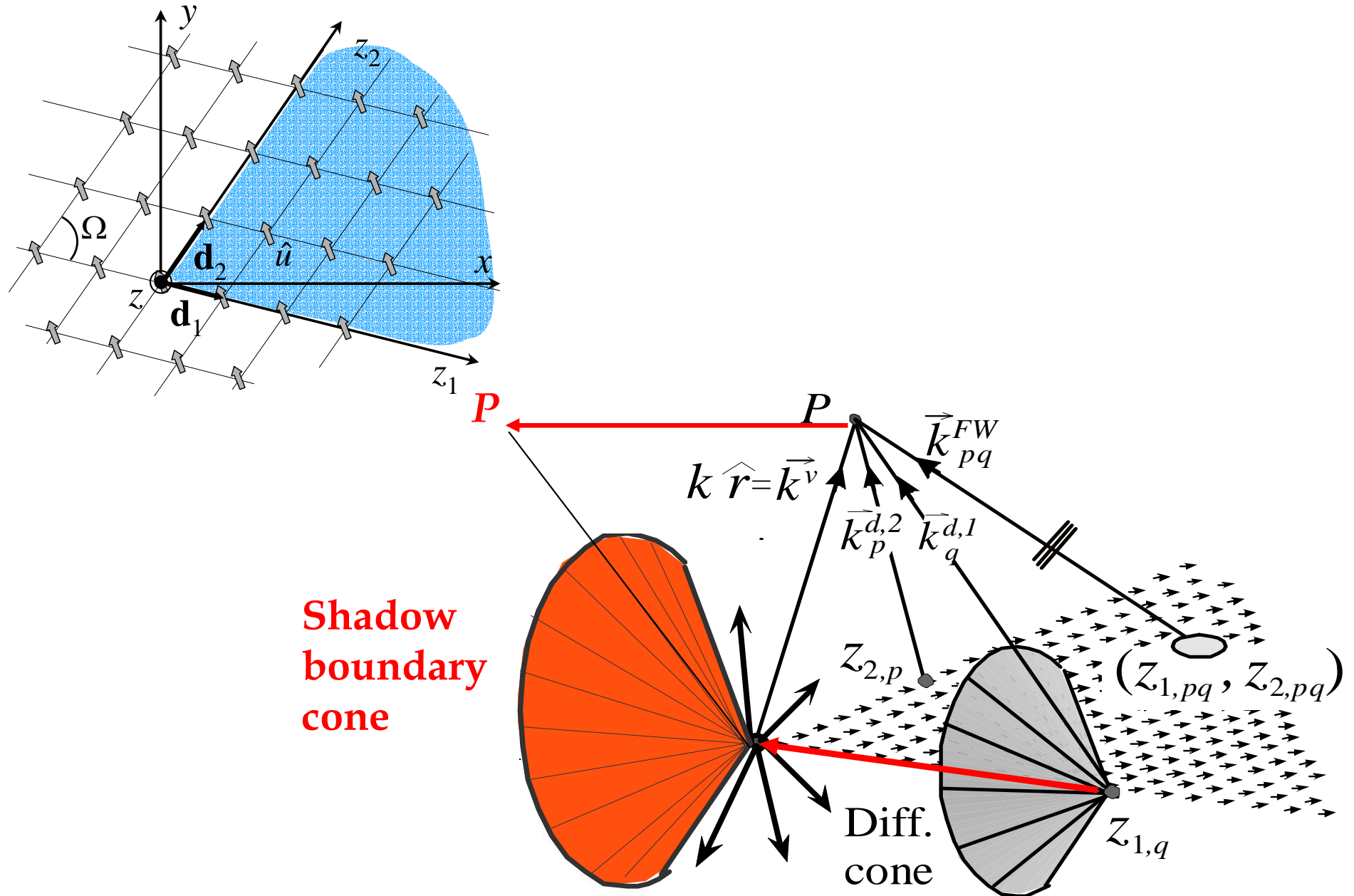


$$\int_{C_\alpha} = \int_{SDP} + 2\pi j \sum \text{Residues}$$



RECTANGULAR ARRAY OF DIPOLES IN FREE SPACE

CANONICAL PROBLEM FOR VERTEX DIFFRACTION: SECTORAL ARRAY



ARRAY OF DIPOLES IN STRATIFIED DIELECTRIC MEDIA

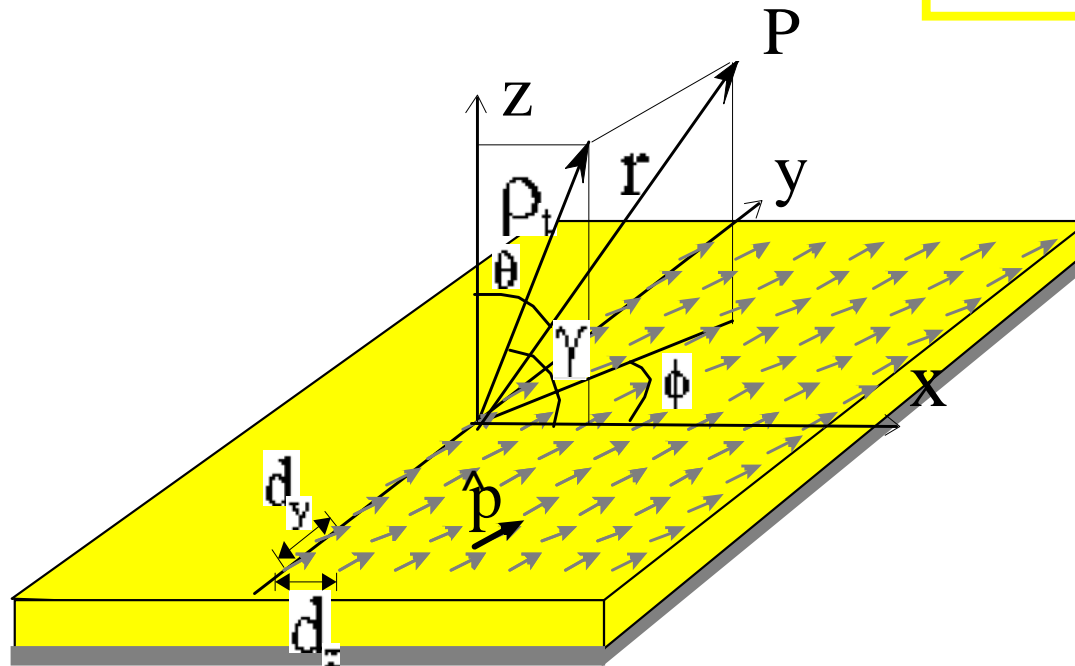
GROUNDED SLAB

$$\vec{A}(P) = \frac{\hat{p}}{2\pi d_y} \sum_{q=-\infty}^{+\infty} \int_{-\infty}^{+\infty} B(k_x) G(\vec{k}_q) e^{-j(\vec{k}_q \cdot \vec{r})} dk_x$$

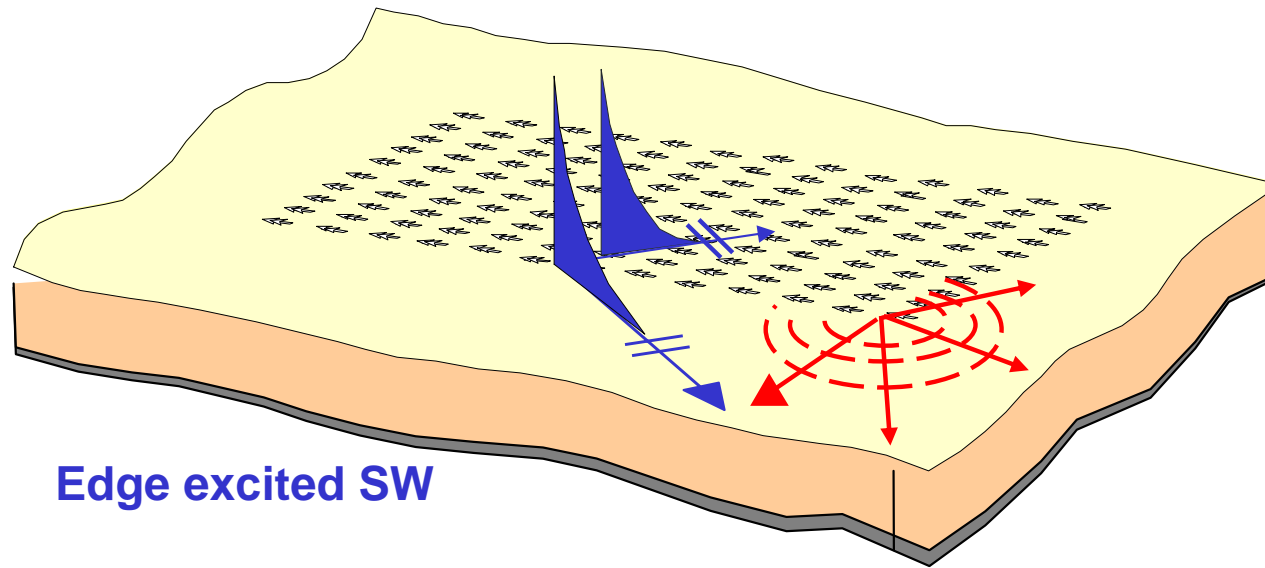
POLES

$$k_{xp} = k_{x0} + \frac{2\pi p}{d_x}$$

The single element Green's function is changed



ARRAY OF DIPOLES IN STRATIFIED DIELECTRIC MEDIA



Edge excited SW

Vertex excited SW

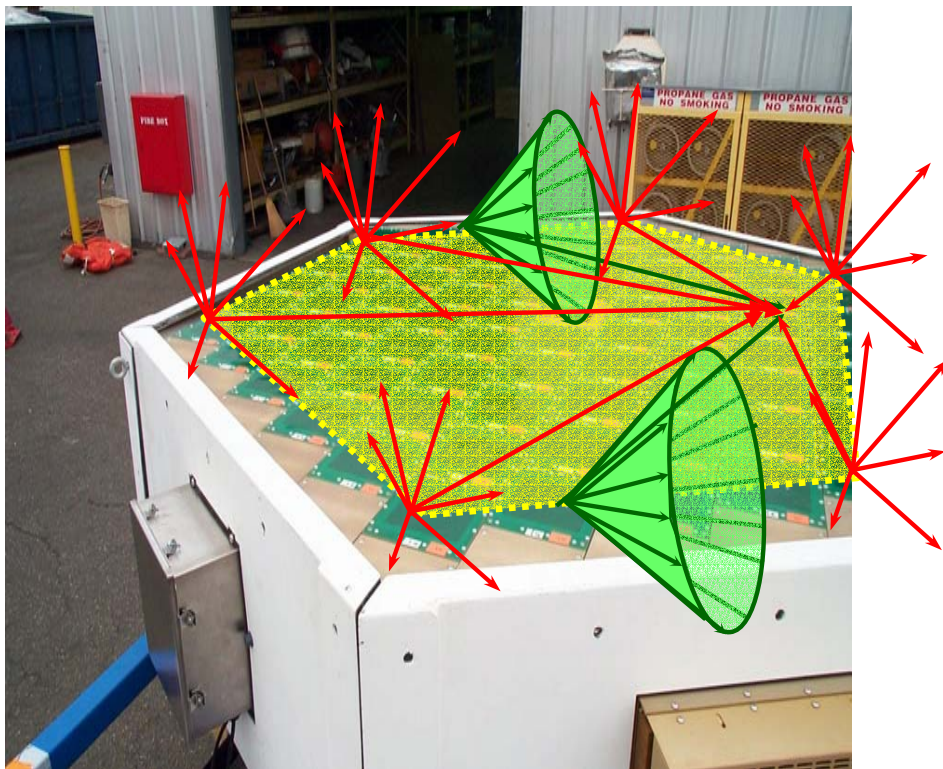
$$\mathbf{E} \approx \sum_{p,q} \mathbf{E}_{pq}^{FW} + \sum_{p,q} \mathbf{E}_{pq}^e + \sum_{p,q} \mathbf{E}_{pq}^v + \sum_{p,q} \mathbf{E}_{pq}^{e,SW} + \sum_{p,q} \mathbf{E}_{pq}^{v,SW}$$

$$\mathbf{E}_{pq}^{e,SW} \approx U_{pq}^{e,SW} e^{-jk_{pq}^{SW} \cdot \mathbf{r}} \quad \mathbf{E}_{pq}^{v,SW} \approx \frac{1}{\sqrt{r}} e^{-jk^{SW} r}$$

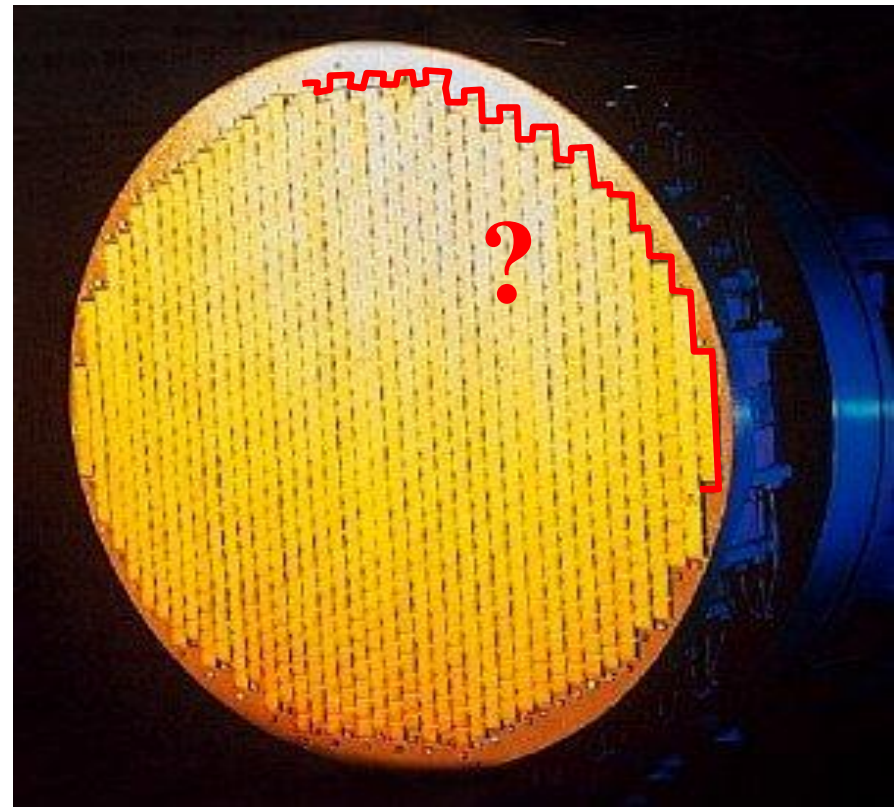
ARBITRARILY CONTOURED ARRAYS

The description in terms of truncated FW has proven to be very efficient for rectangular arrays.

However, as the contour of the array becomes irregular, the number of flash points increases and the contour may no longer be well defined

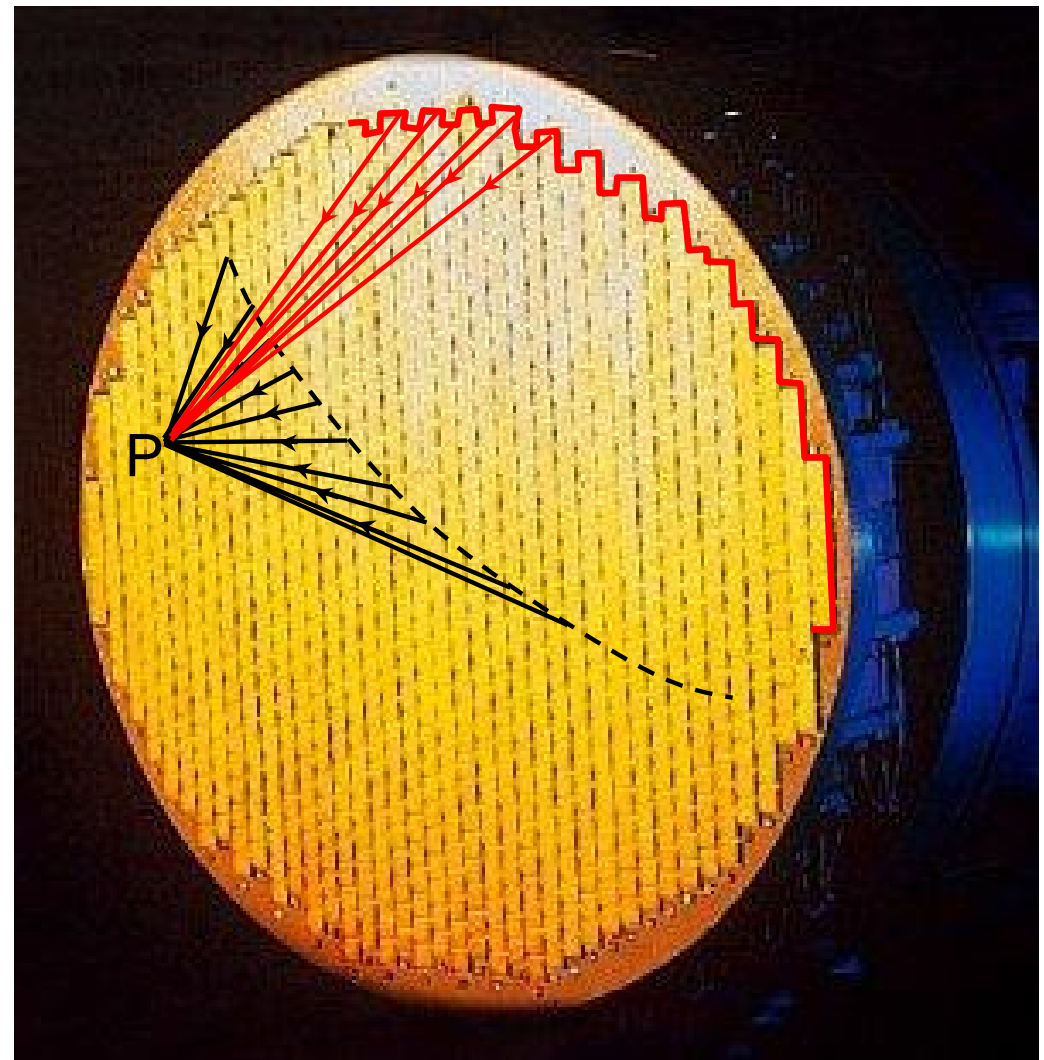
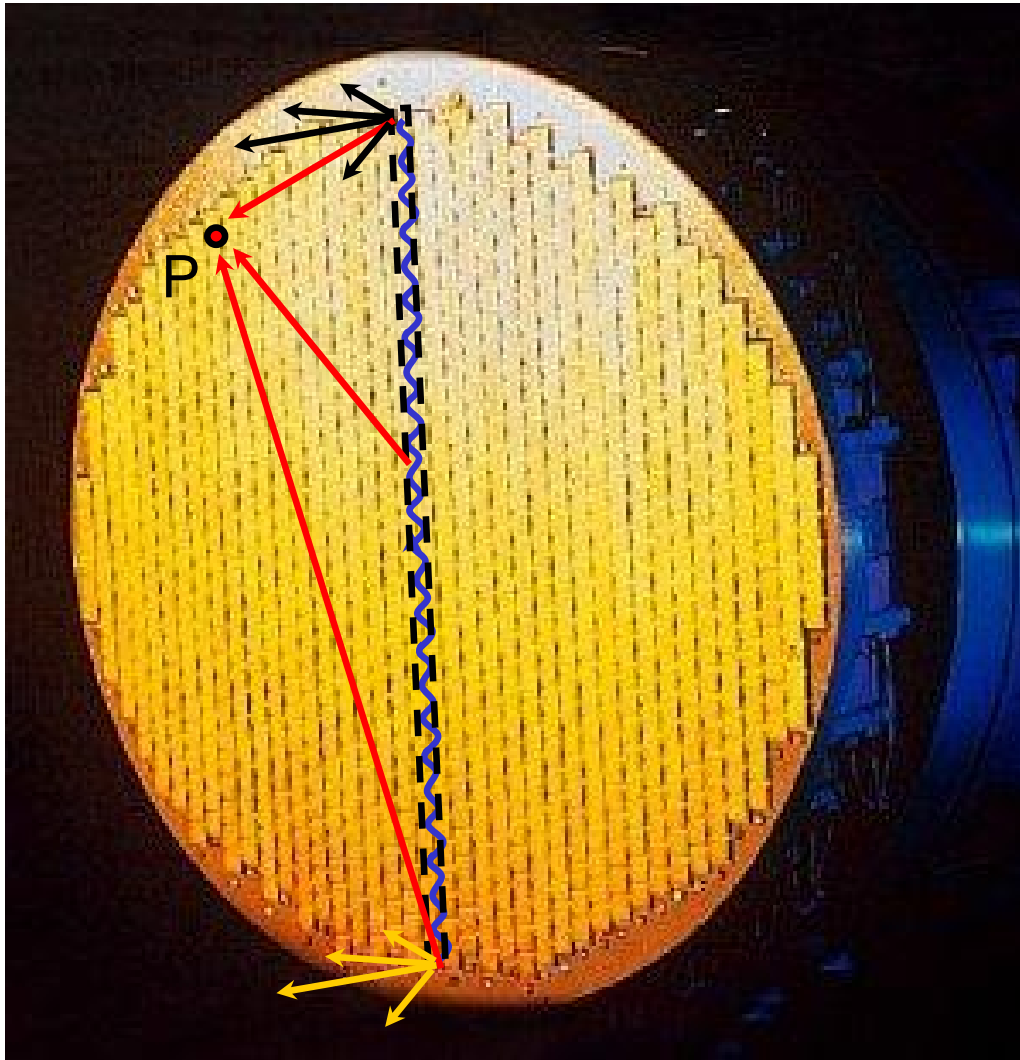


Polygonal contours



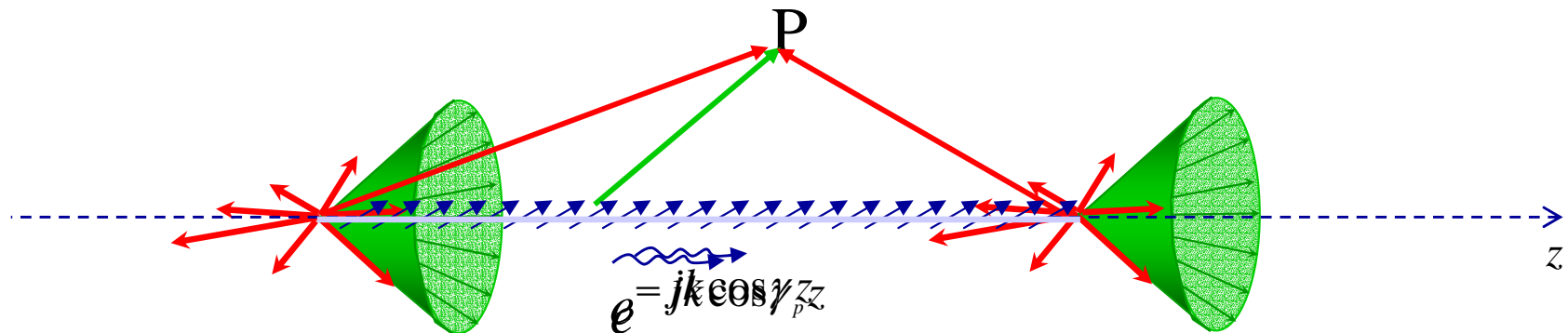
Irregular contours

LINE BY LINE STRATEGY FOR ARBITRARILY CONTOURED ARRAYS

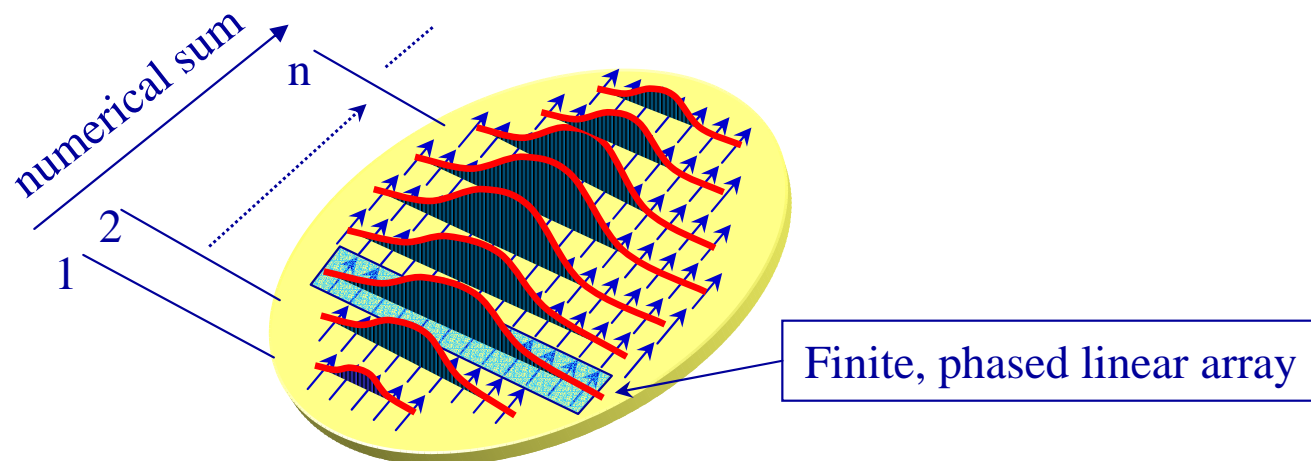


LINE BY LINE STRATEGY FOR ARBITRARILY CONTOURED ARRAYS

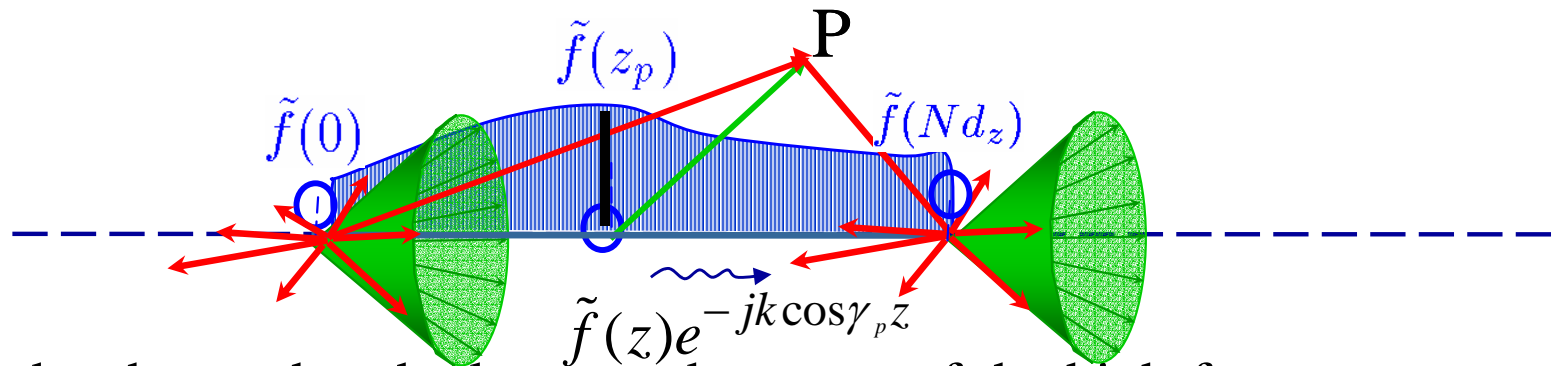
The radiation from a uniform finite linear array can be represented in terms of truncated cylindrical FWs, augmented by the relevant end-point diffracted fields



A uniform planar array radiation can be obtained as a one-dimensional superposition of the dominant high-frequency contributions from the constituting finite phased linear arrays



THE CANONICAL PROBLEM OF THE TAPERED LINE



It can be shown that the lower-order terms of the high-frequency representation of the potential are:

$$A_p(P) = \tilde{f}(z_p) A_p^\infty(P) U(\gamma_p - \beta) + \tilde{f}(z_p) A_p^U(P) + \tilde{f}(0) A_p^R(P) + \tilde{f}(Nd_z) A_p^R(P)$$

$$\propto \frac{e^{-jkr \cos(\beta - \gamma_p)}}{\sqrt{k\rho}} \text{ truncated FW}$$

$$\propto \frac{e^{-jkr}}{kr} \frac{(-1)^p}{(\cos \beta - \cos \gamma_p)}$$

spherical diffracted wave

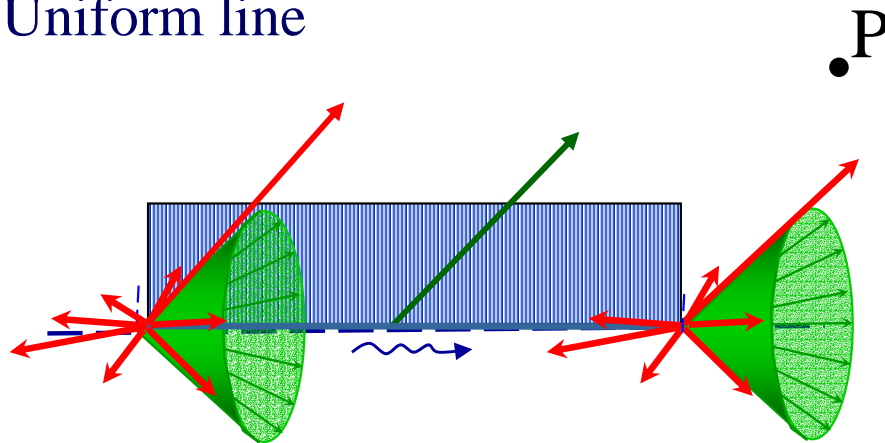
$$\propto \frac{e^{-jkr}}{kr} \frac{(-1)^p}{\sin\left(\frac{\beta - \gamma_p}{2}\right)} \left\{ F \left[2kr \sin^2 \left(\frac{\beta - \gamma_p}{2} \right) \right] - 1 \right\}$$

uniform contribution

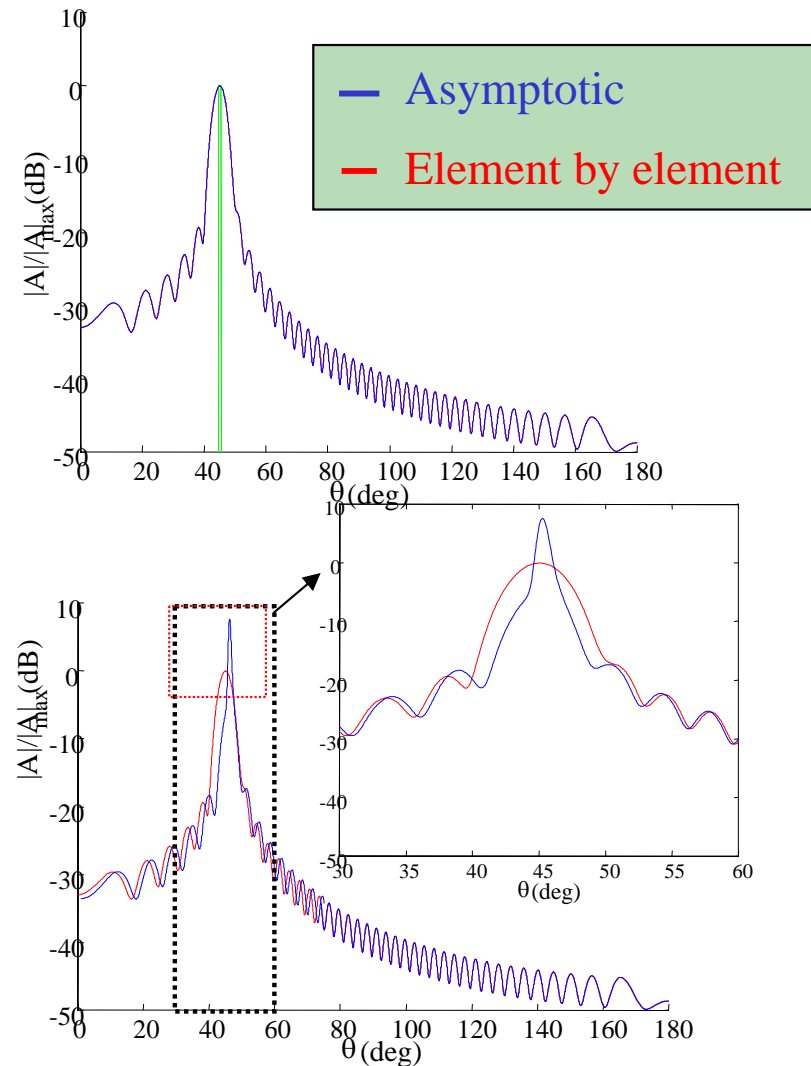
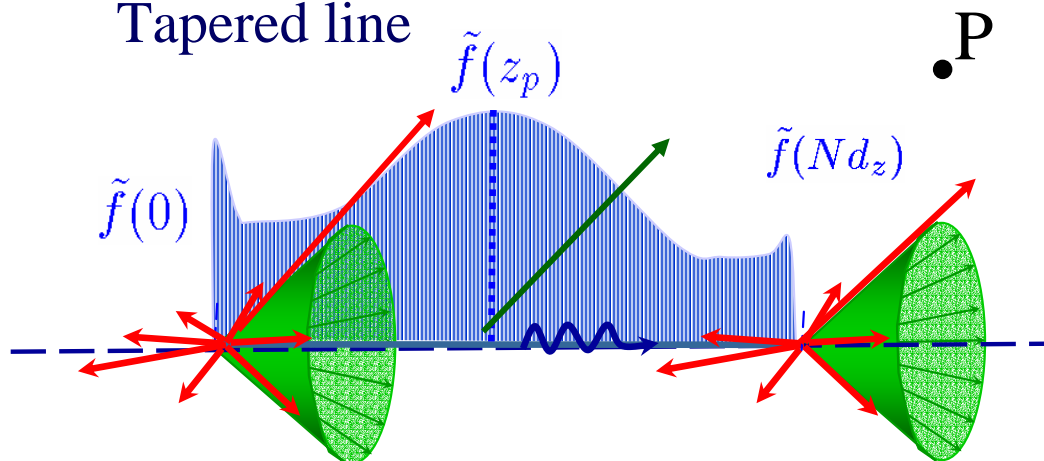
UNIFORM VS. TAPERED LINE

This approach provides excellent results for uniform arrays, both in the near and in the far field regions. Accurate results are obtained also for the field radiated in the near zone by a weakly tapered array. Accuracy, however, decreases when the observation point moves to the far zone.

Uniform line



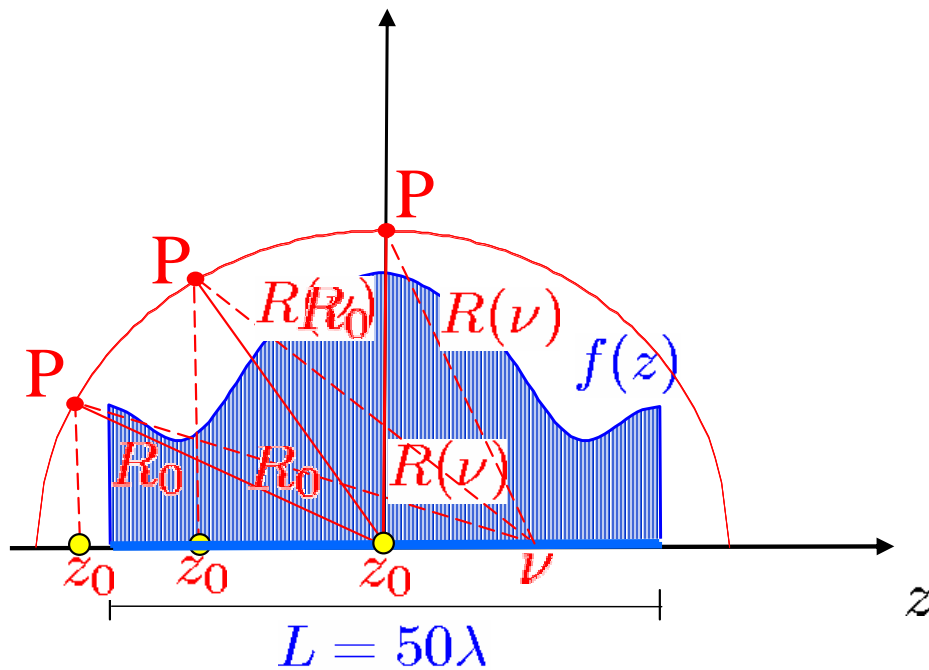
Tapered line



UNIFORM VS. TAPERED LINE

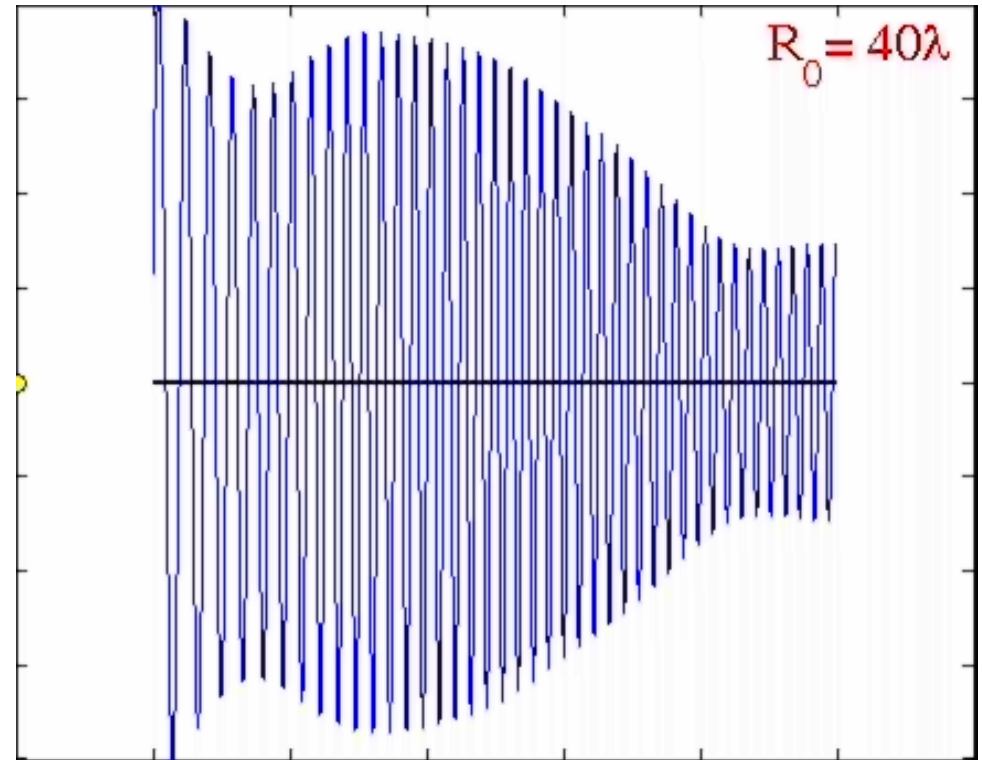
This phenomenon can be clearly explained by observing the behavior of the argument of the radiation integral for different positions of the observer .

- The observer moves in the near field zone.



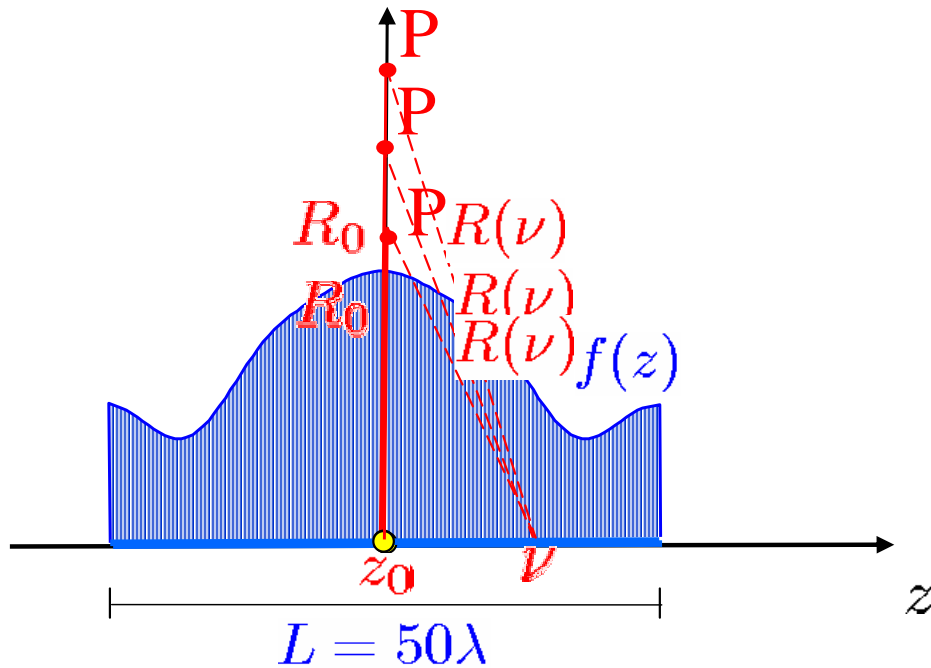
Taylor tapering with $R = 10, \bar{n} = 5$

Integrand function $\frac{e^{-jkR(\nu)}}{4\pi R(\nu)} f(\nu)$



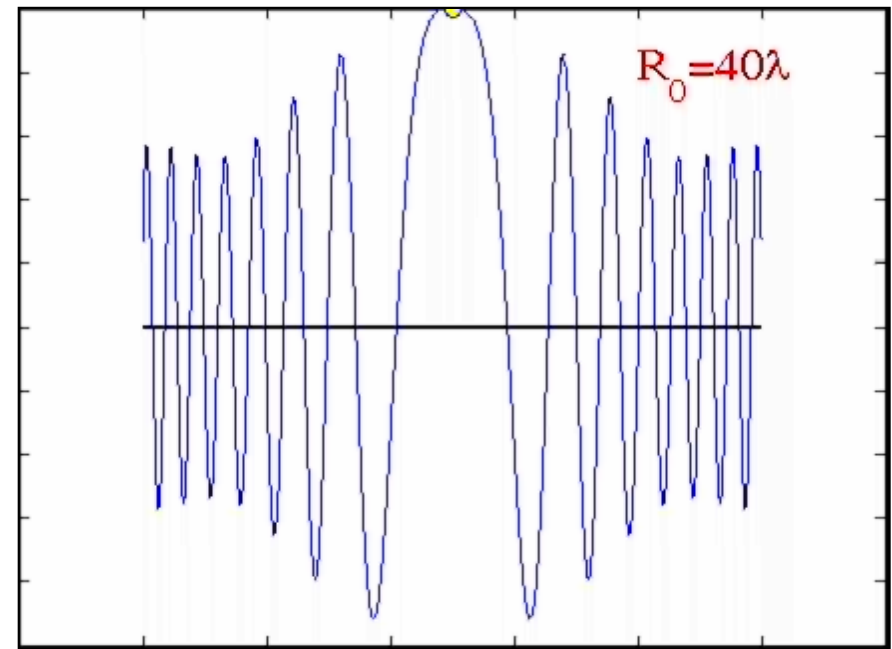
UNIFORM VS. TAPERED LINE

- The observer moves from the near to the far field zone.



Taylor tapering with $R = 10, \bar{n} = 5$

Integrand function $\frac{e^{-jkR(\nu)}}{4\pi R(\nu)} f(\nu)$



The strong localization of radiation contributions is no longer valid for far field observation!

HOW TO OVERCOME THE IMPAIRMENT?

Approximating the actual current distribution through a suitable superimposition of uniform excitations allows to go from the near to the far field region.

This has been done in the past by resorting to DFT or to spatial Fourier Transforms.

- *Nepa, Pathak, Civi, and Chou, 1999*
- *Cicchetti, Faraone, and Balzano, 2003*

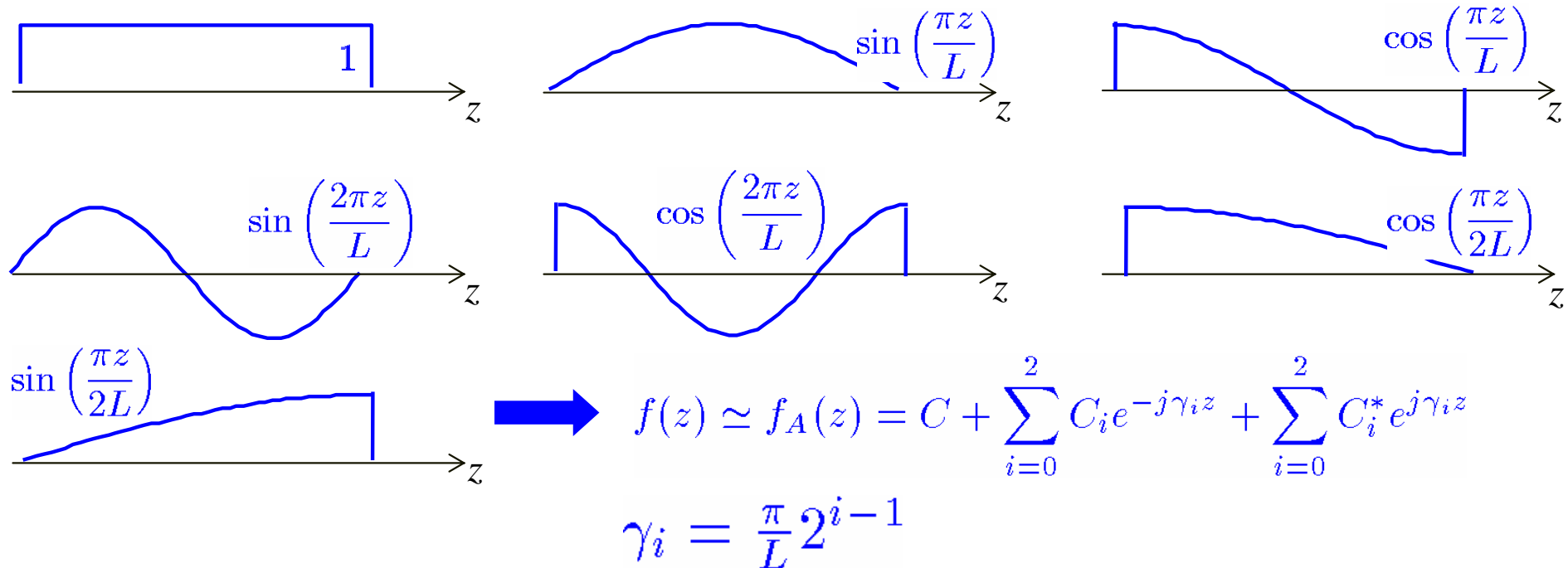
A more efficient representation of the radiated field is obtained by linking the coefficients of the expansion to the characteristics of the actual tapering associated with the dominant asymptotic contributions.

Specifically, the approximate tapering function is defined to match:

- the value and the derivative of $f(z)$ at the two end-points
- the value and the derivative of $f(z)$ at the stationary phase point (if it lies on the line)
- the area subtended by $f(z)$

APPROXIMATION OF THE LINE TAPERING

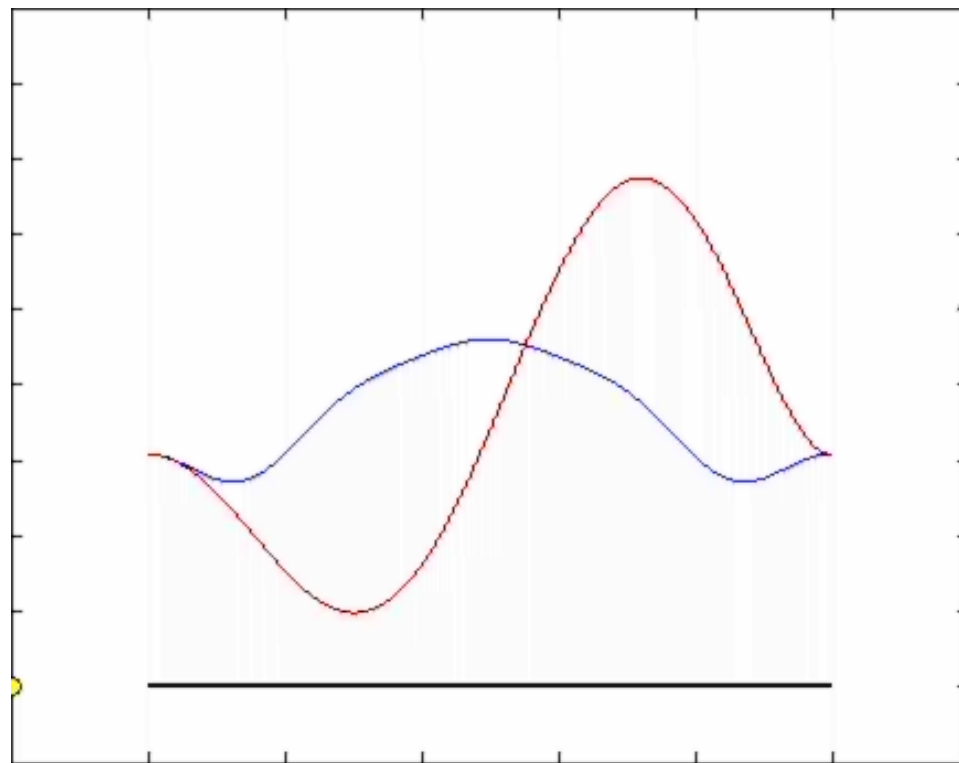
To approximate the current distribution the following set of basis functions is employed, which can be immediately rewritten in terms of equiamplitude linearly phased excitations.



The expression of the expansion coefficients is obtained in closed form by solving a linear system of equations.

APPROXIMATION OF THE LINE TAPERING

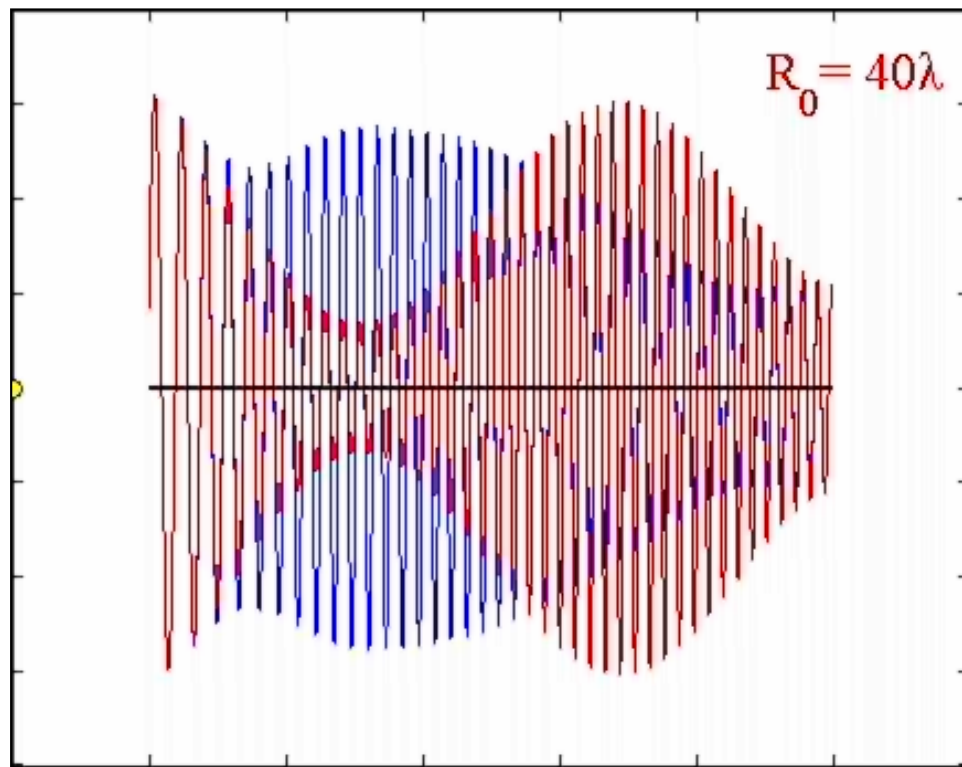
The conditions relevant to the stationary phase point imply a dependence of the equivalent current on the position of the observation point, however they are only required when the stationary phase point lies on the finite line.



- Actual current distribution $f(\nu)$
- Approximated current distribution $f_A(\nu)$
- Stationary phase point

APPROXIMATION OF THE INTEGRAND FUNCTION

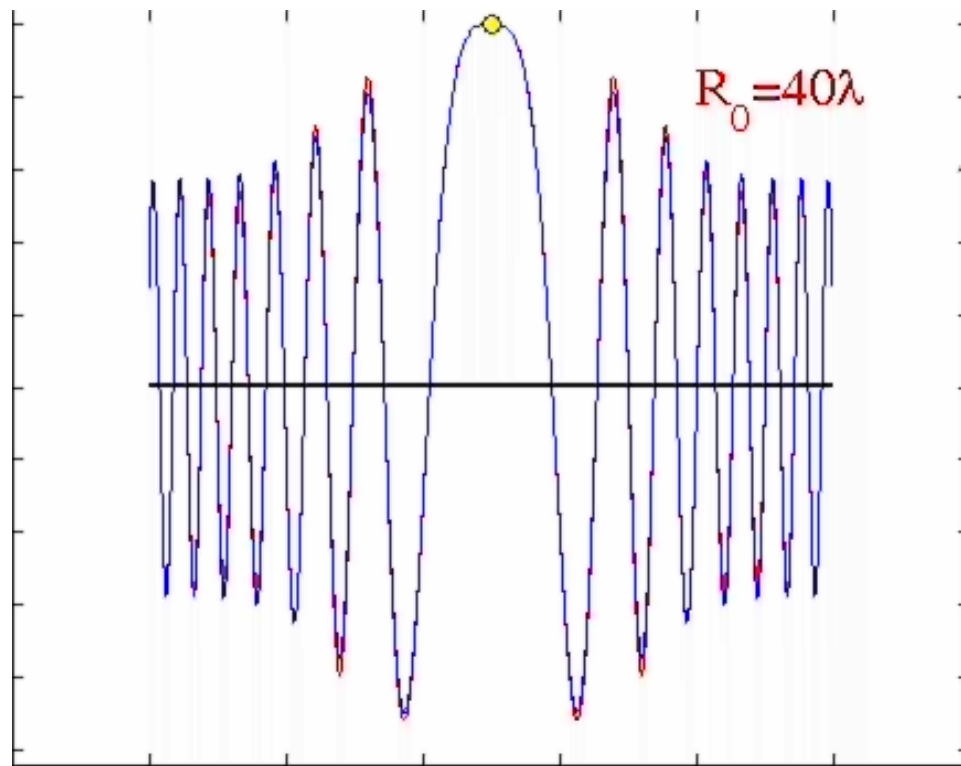
Although the approximated tapering function does not equate the actual current distribution on the whole line, there is a good agreement between the relevant radiation integrals:



- Actual integrand $\frac{e^{-jkR}}{4\pi R} f(\nu)$
- Approximated integrand $\frac{e^{-jkR}}{4\pi R} f_A(\nu)$
- Stationary phase point

APPROXIMATION OF THE INTEGRAND FUNCTION

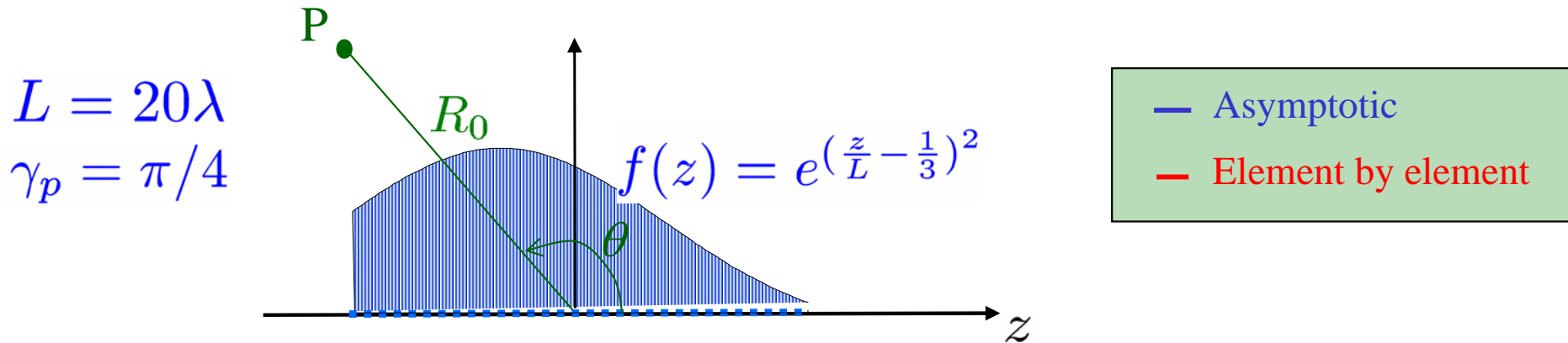
Thanks to the condition on the subtended area, the agreement between the relevant radiation integrals is preserved when the observation point moves to the far field region



- Actual integrand $\frac{e^{-jkR}}{4\pi R} f(\nu)$
- Approximated integrand $\frac{e^{-jkR}}{4\pi R} f_A(\nu)$
- Stationary phase point

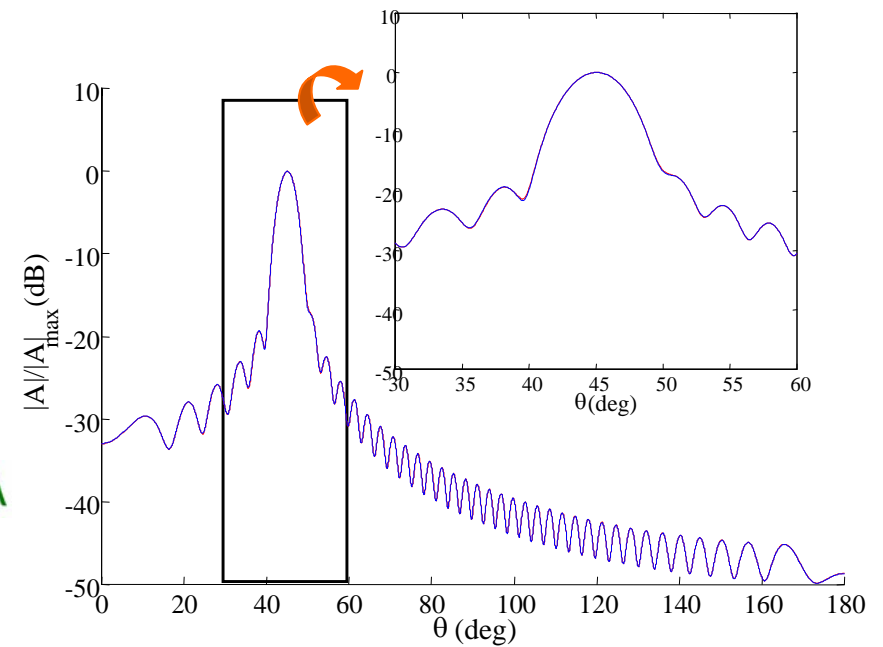
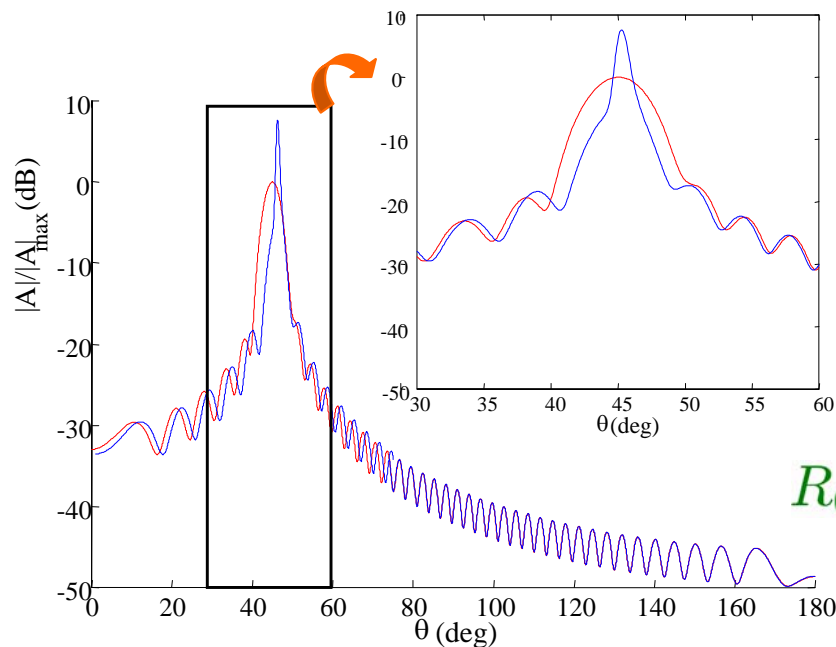
A COMPARISON OF THE TWO APPROACHES

Numerical results confirm that the proposed approach yields more accurate results when the observation point approaches the far field region:



Actual current

Approximated current



LINEAR ARRAY SYNTHESIS

Tapered linear array

Poisson

\sum_p tapered continuous lines

$$\sum_{n=0}^{\infty} f(nd_z) e^{-jk_z nd} \frac{e^{-jkR_n}}{4\pi R_n}$$

$$\sum_{p=-\infty}^{+\infty} \int f(z) e^{-jk_z p z} \frac{e^{-jkR(z)}}{4\pi dR(z)} dz$$

Propagating modes

$$f(z) \simeq C_{0p} + \sum_{m=1}^3 C_{mp} e^{j \frac{2\pi}{L2^{m-1}}} + \sum_{m=1}^3 C_{mp}^* e^{-j \frac{2\pi}{L2^{m-1}}}$$

Coefficients are chosen to match:

- the value and the first derivative of f at the end-points and at the saddle point
- the area subtended by f to the line

\leftarrow_m uniform continuous lines

Evanescent modes

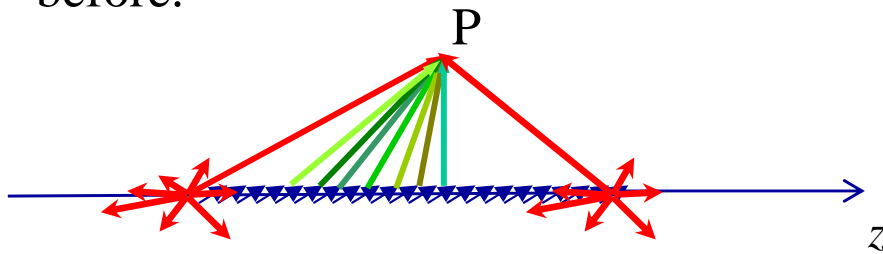
$$f(z) \simeq C_0 + \sum_{m=1}^2 C_m e^{j \frac{2\pi}{L2^{m-1}}} + \sum_{m=1}^2 C_m^* e^{-j \frac{2\pi}{L2^{m-1}}}$$

Coefficients are chosen to match:

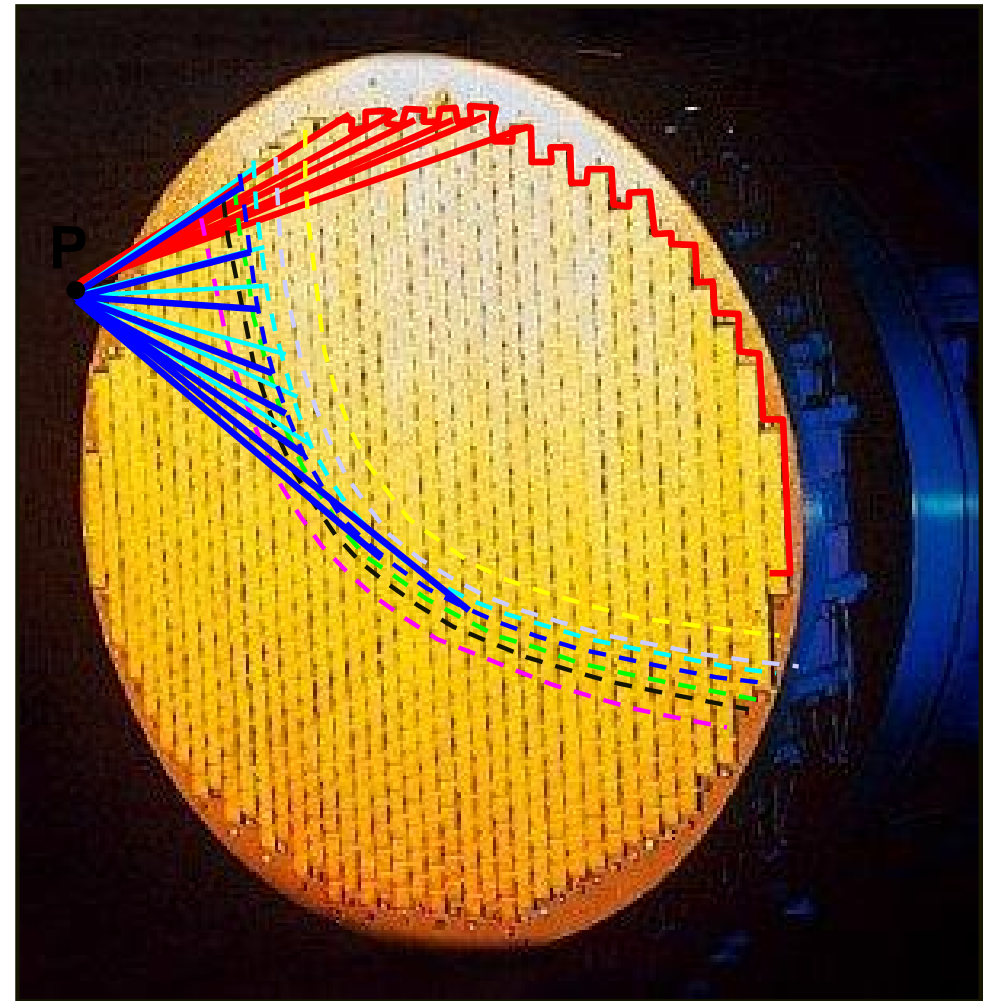
- the value and the first derivative of f at the end-points

PLANAR ARRAY SYNTHESIS

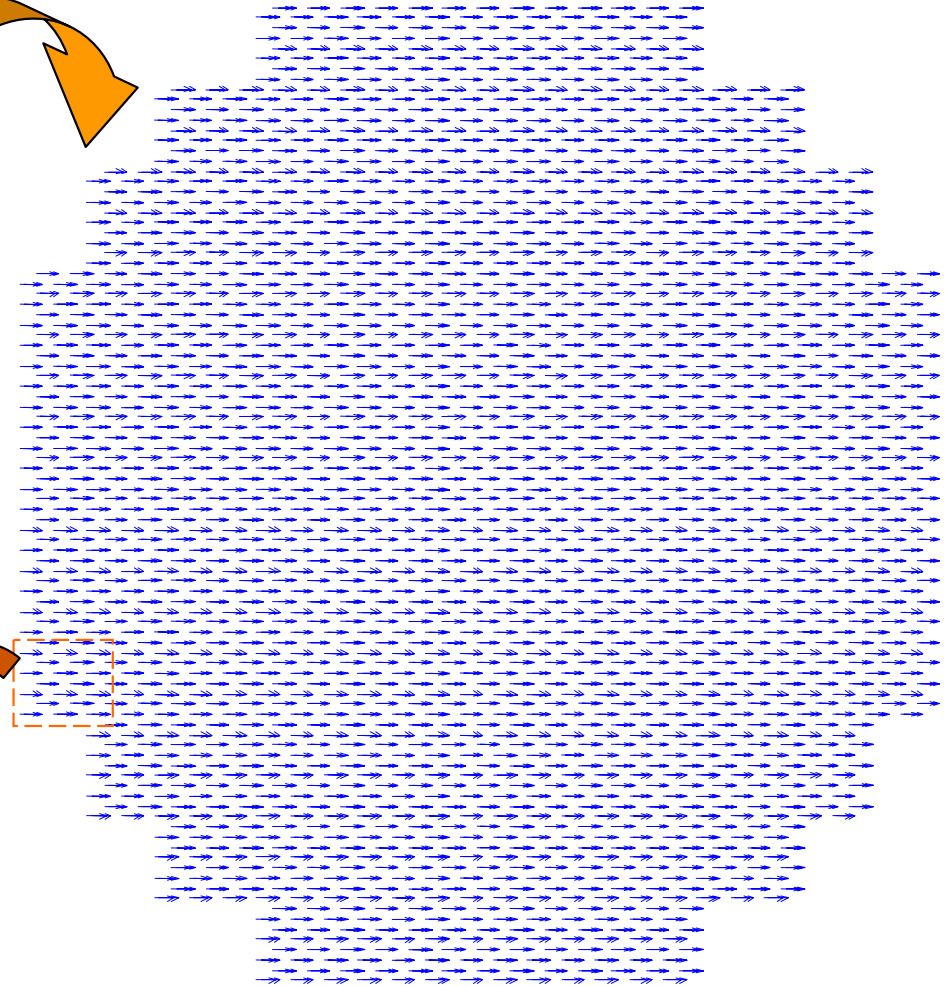
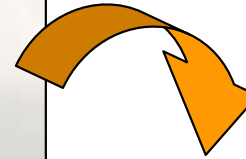
- The radiation from the planar array is reconstructed by numerical summation of the linear arrays contributions.
- These contributions are uniformly asymptotically evaluated as shown before.



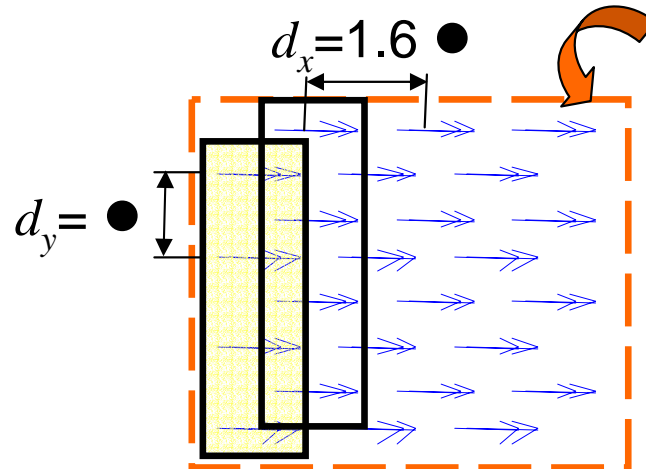
- Finally, the field radiated by the planar array is represented as the sum of diffracted fields from the actual rim plus (when needed) a limited number of conical waves arising from points located on the array surface.



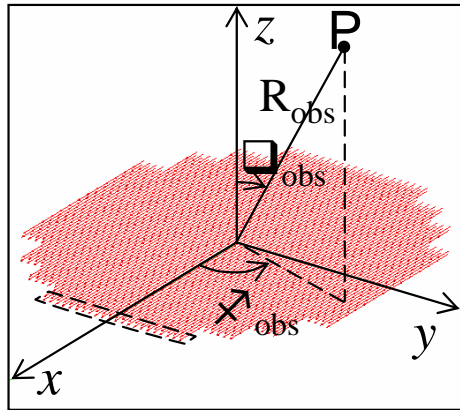
NUMERICAL RESULTS: ARRAY CONFIGURATION



Array of 2160 elementary magnetic dipoles



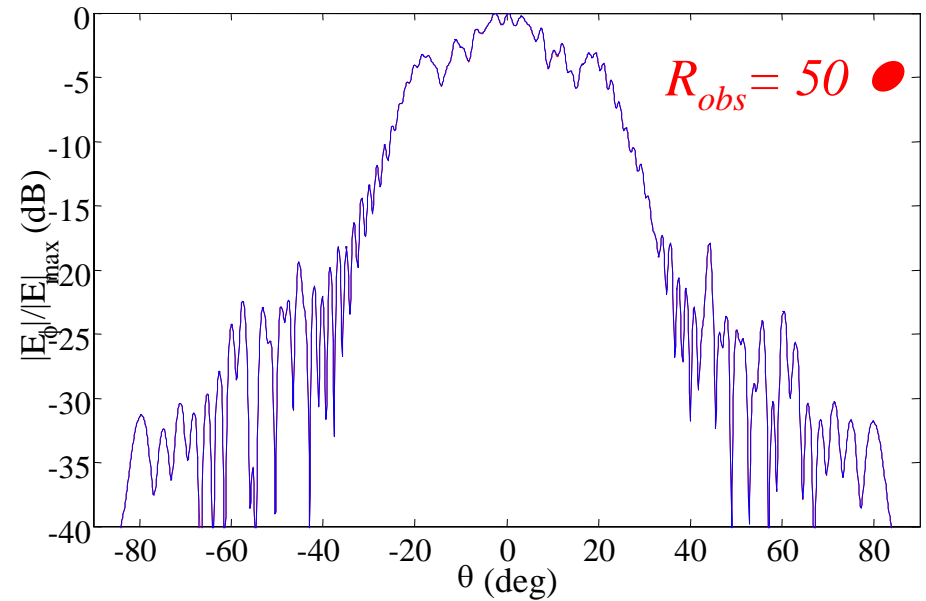
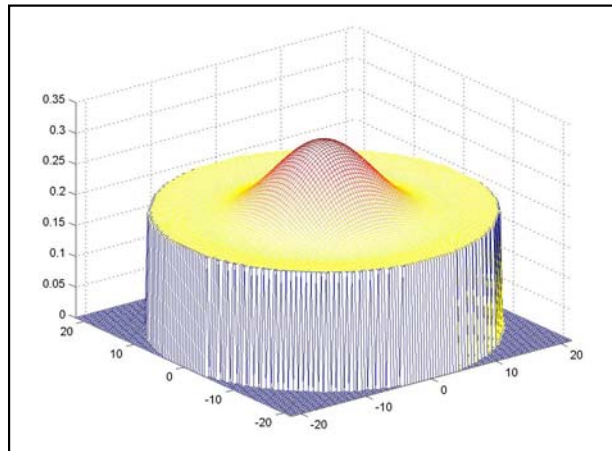
NUMERICAL RESULTS: FREE SPACE RADIATION



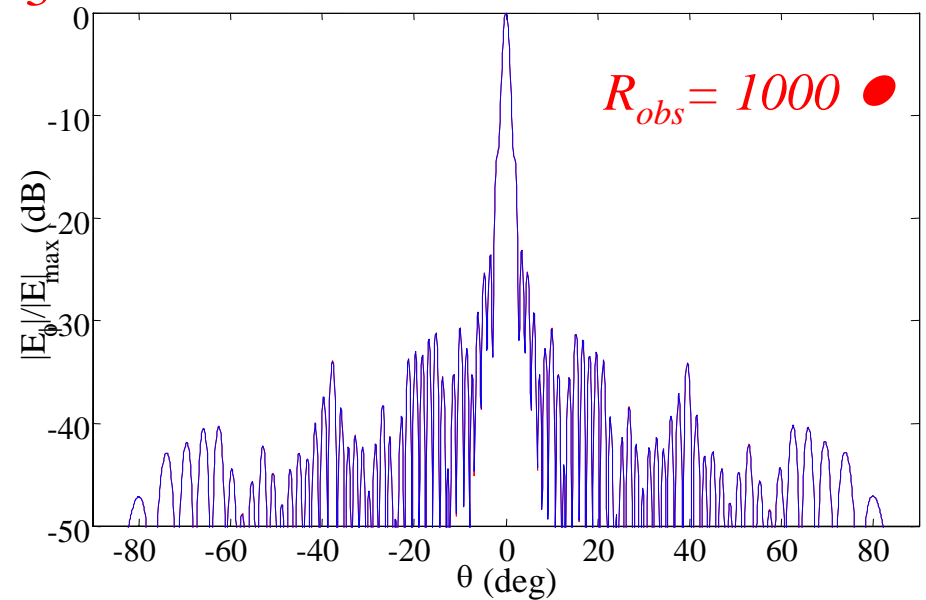
Bearing angles: $\alpha_0=0^\circ$, $\varphi_0=0^\circ$

Observation plane: $\varphi_{obs}=0^\circ$

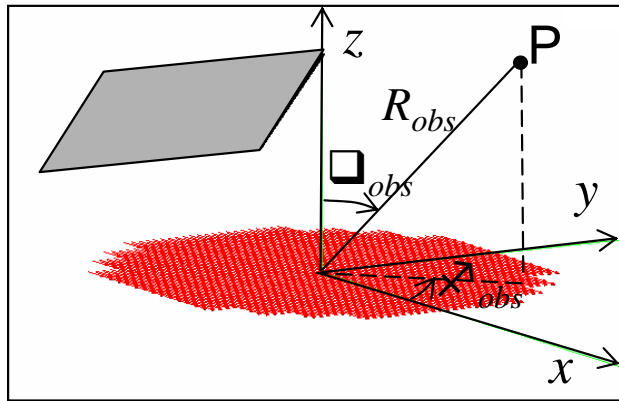
Taylor distribution with SLL = 20dB and $n = 3$



— Line by line
— Element by element



NUMERICAL RESULTS: INTERACTION WITH THE ENVIRONMENT

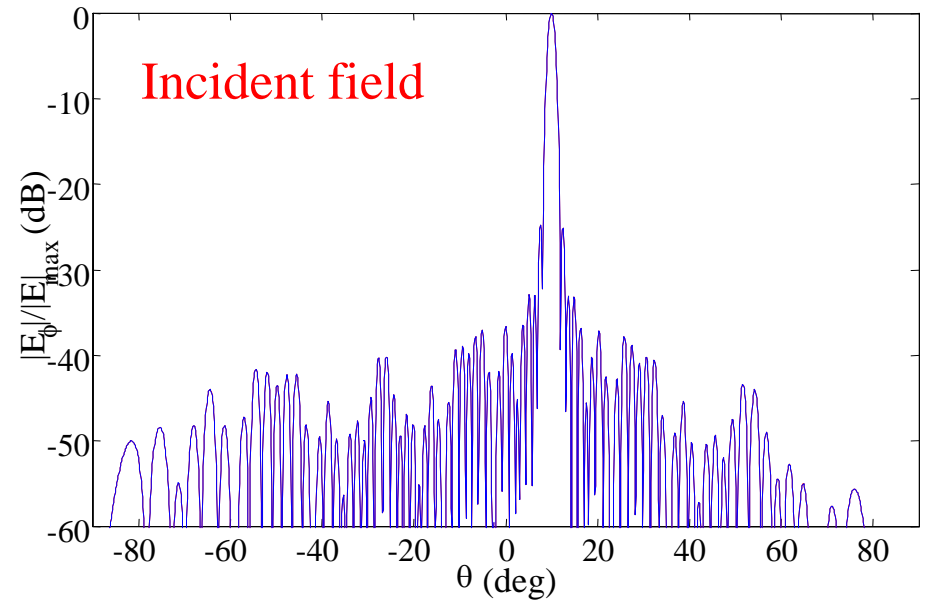
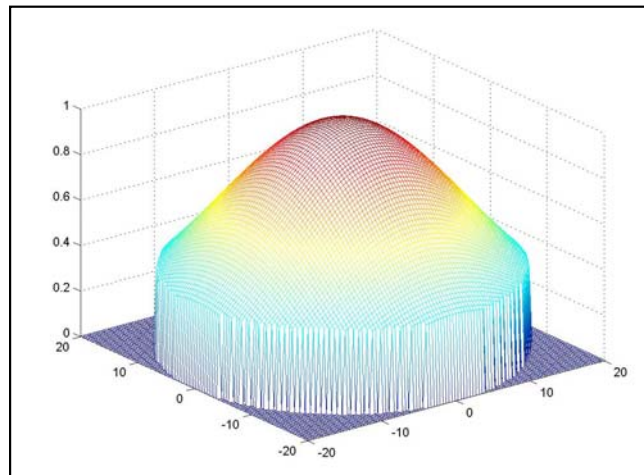


Bearing angles: $\alpha_0 = 10^\circ$, $\varphi_0 = 0^\circ$

Observation: $\varphi_{obs} = 0^\circ$, $R_{obs} = 10000$ ●

Gaussian distribution with $\diamond = 14$ ●

24 ● x 17 ● PEC plate



— Line by line + DFT
— FEKO (Element by element + PO)

